CHAPTER 1: Introduction and Literature Review

1.1 Introduction

Frustration is ubiquitous in nature and a fascinating topic for physicists due to their complexity and diverse behavior. It is defined by the inability of a system to satisfy all interactions simultaneously and thus select a degenerate ground state which is unique in comparison to ordered state of matter [1]. Frustration is a unifying theme in the complex natural systems e.g. the immune system, the brain, protein folding, and systems that evolve and adapt [2]–[5]. Frustration was initially identified in crystalline water ice, which retains a 'frozen-in' disorder state down to extremely low temperature, showing the characteristic of residual or zero point entropy. Initially, the structure of water ice was considered being composes of tetrahedrally coordinated molecules without any consideration of hydrogen atom position [6]. In 1933, Giauque and co-workers precisely measured the low temperature residual entropy of water ice [7], [8], which enable Pauling to propose the famous explanation about the inequality between crystal symmetry and bonding necessities of water molecules [9]. He predicted a unique type of local proton disordering the so-called "ice rules", as anticipated by Bernal and Fowler [10]. It has been proposed Bernal and Fowler that the crystal structure of hydrogen-bonded water molecules (H_2O) consists of a network of corner shared tetrahedra, in which the protons are at the apexes whereas oxygen ion situated at the centre. In these corner shared tetrahedra, two protons are relatively closer to the central oxygen ion, in comparison to the remaining two. Pauling showed that 'ice rule' prevent the proton ordering and gives "microscopically degenerate" ground state. The estimated ground state degeneracy for N number of water molecules to be ~ $(3/2)^{N/2}$ thus giving the residual

ground state entropy (S_0) ≈(R/2)ln(3/2), where R is the molar gas constant. This estimated entropy matches well with the experimental results [7], [11] which was later confirmed by the neutron diffraction measurements as well [12].

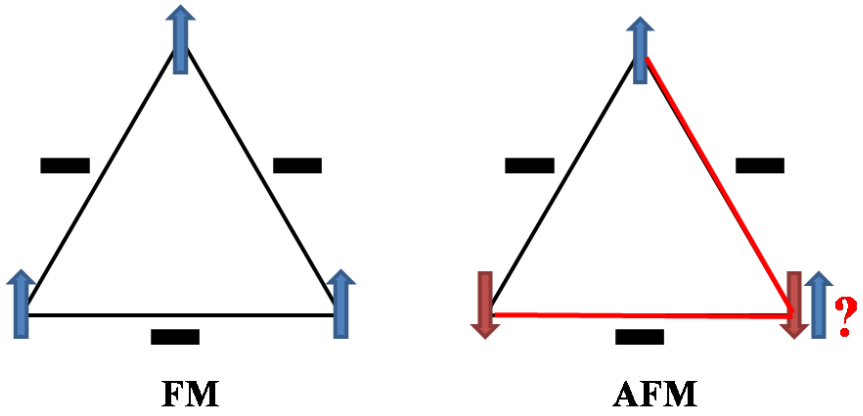

Figure 1.1: (left) Ferromagnetically and (right) antiferromagnetically coupled Ising spin arranged on a triangle.

To study the frustration one of the highly successful approach is to study the frustrated magnetic system [13]. Much like the atomic arrangement in solids, liquid and gaseous phases of the matter, magnetic moments forms magnetically ordered, spin glass, spin liquids, spin ice, and paramagnetic phases in magnetic systems,. Study of frustration induced different phases of magnetism is a profound area in condenses matter and material's physics. To understand the magnetic frustration; the easiest example is two states Ising spin, which can point in only two possible directions, residing at the vertex of an equilateral triangle having antiferromagnetic interaction [14]. Figure 1.1 shows the ferromagnetic (FM) and antiferromagnetic (AFM) exchange interactions between the Ising spins. In case of FM interaction, all spins are directed in a single up (or down) direction and satisfied the pairwise

nearest neighbor ferromagnetic (FM) interaction. When a group of triangles is condensed to form an edge-shared triangular lattice, they form a non-frustrated long range ordered state at finite temperature.

On the other hand, in case of AFM exchange interaction, it is impossible that all three spins lie at the vertex of the triangle to align mutually anti-parallel to each other hence do not satisfy all pairwise interaction pair by pair. Due to failure of pairwise interaction, ground state energy cannot be minimized and thus gives a unique 6 fold degenerate ground state instead of the non-degenerate ground state. Figure 1.2 shows all six possible degenerate states in a given triangle. In triangular lattice formed by edge-sharing, this degeneracy becomes massive and in turn gives a huge configurational spin disorder which inhibits the development of a long-range ordered state. At low temperature, these spin fluctuations are governed by quantum or thermal phenomenon without any long-range ordered phase or phase transition thus exhibits a large residual 0K magnetic entropy [15], [16].

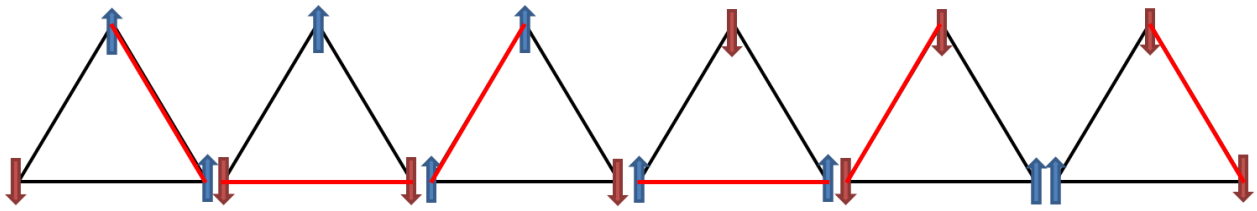

Figure 1.2: 6-fold degeneracy in antiferromagnetically coupled Ising spin in triangular lattice.

The above example of magnetic frustration is known as geometric frustration, where positions of the magnetic ion are fixed at their regular periodic positions in the lattice. The magnetic frustration is also observed in the non-periodic lattice where positions of the

magnetic ion do not follow the periodic translational symmetry. Due to this randomness, competition between two or more than two interaction produces the ground state degeneracy in the system. The well-known example of random frustration is AuFe where magnetic Fe ion is substituted in the Au metal matrix [17]. In this system, depending on the separation between the substituted magnetic Fe ions, J_{RKKY} interaction acting between two Fe moments mediated by conduction electron termed as Ruderman–Kittel–Kasuya–Yosida (RKKY) interaction, which can be either antiferromagnetic or ferromagnetic. Due to the presence of both antiferromagnetic and ferromagnetic interaction, frustration arises in AuFe system. This kind of frustration is known as random frustration being the fundamental ingredient in the physics of spin glass materials [18].

1.2 Geometrical magnetic frustration

Following the discovery of high temperature superconductivity, search for novel strongly correlated systems becomes a high priority research area. In 1973, Anderson [19] proposed that in high temperature superconductors resonating valance bond state could be replaced by antiferromagnetic Neel ordering. In this direction, one of the highly successful approaches has been the study of highly frustrated magnetic (HFM) systems. Due to the large degeneracy of the ground state, the HFM systems do not show long range ordered state even at 0K and retain a highly disordered or frustrated state. The degree of frustration of frustrated magnetic system are defined by the frustration index (f) [20], defined as

$$f = \Theta_{CW}/T_{min} \qquad (1.1)$$

Where, Θ_{CW} is the Curie-Weiss temperature and T_{min} is the minimum temperature at which system pertain the disordered state. For ordered system f~1, whereas for highly frustrated

magnetic system f >>1 i.e. Θ_{CW} is much larger than ordering temperature T_{min}. Due to lack of magnetic ordering, HFM systems are extremely sensitive to small perturbations and quantum mechanical effects, hence their propensity to exhibits exotic behaviors [16]. Experimental findings suggest that most of the HFM systems are geometrically frustrated, in which lattice architecture prevents the long-range magnetic ordering associated with ferromagnetic or antiferromagnetic interactions [13], [17]. These lattices mainly consist of condensation of massive triangles or tetrahedral. The examples of the geometrically frustrated lattice are; kagome, triangular, hyperkagome, garnets, and pyrochlore, etc. Kagome and triangular lattice are 2-d lattices consist of corner and edge-sharing of triangles. The hyperkagome and garnet lattices are formed by the network of the corner-sharing triangle in 3-dimensions whereas pyrochlore lattice consists of corner-sharing of tetrahedra [16], [21].

Out of several magnetic oxides, pyrochlore oxides are most studies materials due to their exceptionally high compositional diversity and structural flexibility thus providing a remarkable variety of properties and applications such as geometrically frustrated magnetism [16], [22]–[24], giant magnetoresistance [25], ferroelectricity [26], photocatalysis [27], photoluminescence [28], magneto-optical [29]–[31], solid oxide fuel cell [32]–[34] etc. The chemical formula of pyrochlore oxides is $A_2B_2O_7$, where A cation is trivalent and B cation is tetravalent. In the context of magnetic frustration, cubic pyrochlore oxides have attracted tremendous attention because the A and B site lies at two different interpenetrating lattices of corner shared tetrahedra as shown in figure 1.3. Depending on the magnetic and non-magnetic nature of A and B cations, pyrochlore oxides show a diverse variety of exotic phenomena associated with magnetic frustration [17].

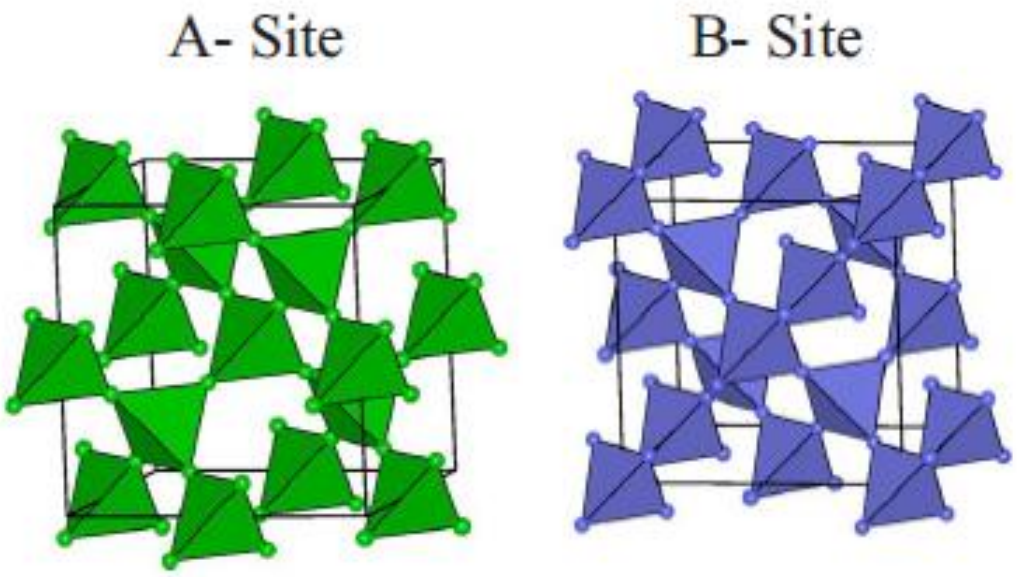

Figure1.3: Formation of corner-shared tetrahedra by A and B sites in cubic pyrochlore oxides. [17]

1.3 Magnetic rare earth pyrochlore oxides

Magnetic rare earth pyrochlore oxides consist of magnetic rare earth (RE) at A-site whereas B-site is mostly non-magnetic. Thus, depending on the rare earth ion diverse verity of low temperature exotic magnetic behavior ranging from conventional long-range antiferromagnetic ordering ($Gd_2Ti_2O_7$) [35], [36], spin glass freezing ($Y_2Mo_2O_7$) [37], thermal and/or quantum order-by-disorder phenomena ($Er_2Ti_2O_7$) [38], spin liquid behavior ($Tb_2Ti_2O_7$) [16], [24] and spin ice phenomena ($Ho_2Ti_2O_7$ and $Dy_2Ti_2O_7$) [22], [23] have been observed. The focus of the present thesis on the complex dielectric and magnetic behavior of $Ho_2Ti_2O_7$ and $Dy_2Ti_2O_7$ spin ices. The underlying spin ice phenomenology and its associated complex behavior in these compounds are explained as follows.

1.4 Spin Ice phenomenology and spin ice materials

In 1997, for the first time Harris et al. [39], discovered the spin ice phenomenology in $Ho_2Ti_2O_7$ (HTO) compound. Their investigation concludes that in HTO local crystal field anisotropy leads the magnetic frustration in spite of effective ferromagnetic interaction. Calculations suggest the formation of "2in-2out" spin configuration of Ising spin in each corner shared tetrahedra, similar to the proton arrangement in water ice, due to which Harris et al. termed this system as 'spin ice". Further, muon spin resonance and neutron scattering studies shows the absence of magnetic ordering down to 50 mK, making this system highly frustrated having a frustration index f ~100 [40]. Later, similar behavior have been observed in $Dy_2Ti_2O_7$ (DTO) [22], [41], $Ho_2Sn_2O_7$ [42], as well, which show the disordered spin ice behavior at low temperatures.

In 1999, Ramirez et al. [22] performed low temperature magnetic and specific heat measurement on DTO. In temperature dependent magnetization no evidence of magnetic ordering was observed despite a small positive Curie-Weiss temperature Θ_{CW} ~ 0.5 K as obtained from inverse of χ_{dc} (T) as shown in the inset of figure 1.4 (a). The lack of magnetic ordering was further observed in temperature dependent specific heat, C (T) measurement consistent with the magnetic frustration assisted random spin freezing in DTO. The deduced value of magnetic entropy shows Rln(3/2) of residual zero point entropy as shown in figure 1.4 (b).

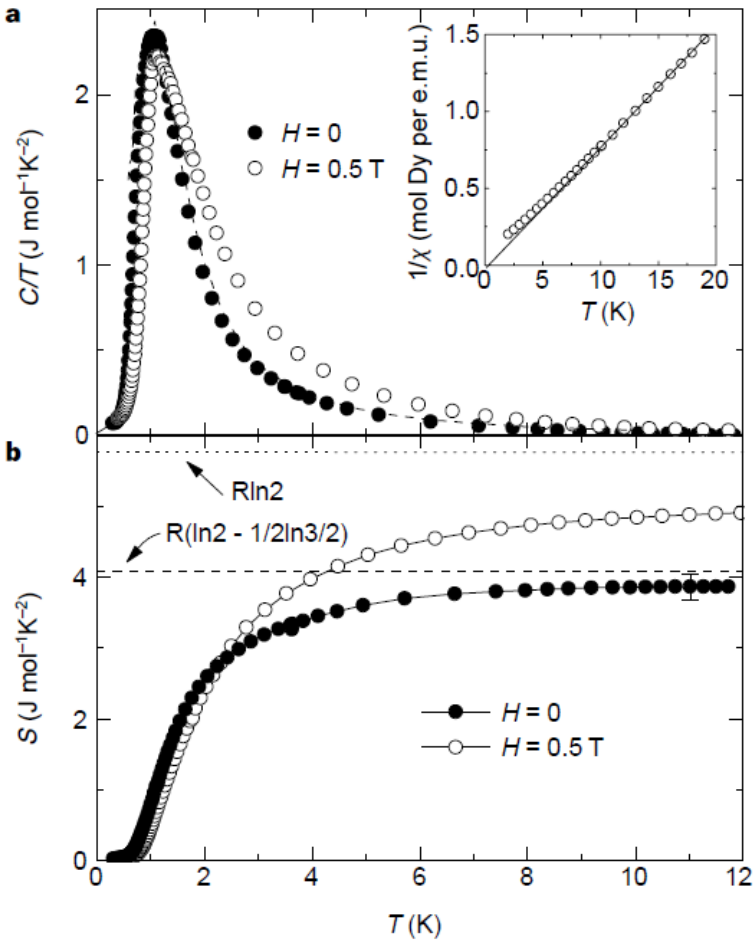

Figure 1.4: Temperature dependent; (a) specific heat and (b) entropy of $Dy_2Ti_2O_7$ measured at 0 T and 0.5 T magnetic field, showing the similarity with Pauling predicted water ice entropy R(ln2 – 1/2ln3/2). [22]

The so observed magnetic entropy is equal to the entropy of the frustrated water ice as obtained by Pauling [9]. On the basis of this similarity, Ramirez et al. (1999) suggested that similar to proton arrangement in water ice, magnetic ion form a network of corner shared tetrahedra in which each spin is directed towards the center of tetrahedra in these compounds. At low temperature, due to effective ferromagnetic interaction, each tetrahedra form a macroscopically degenerate "2in-2out" spin structure as shown in figure 1.5 [22], [43].

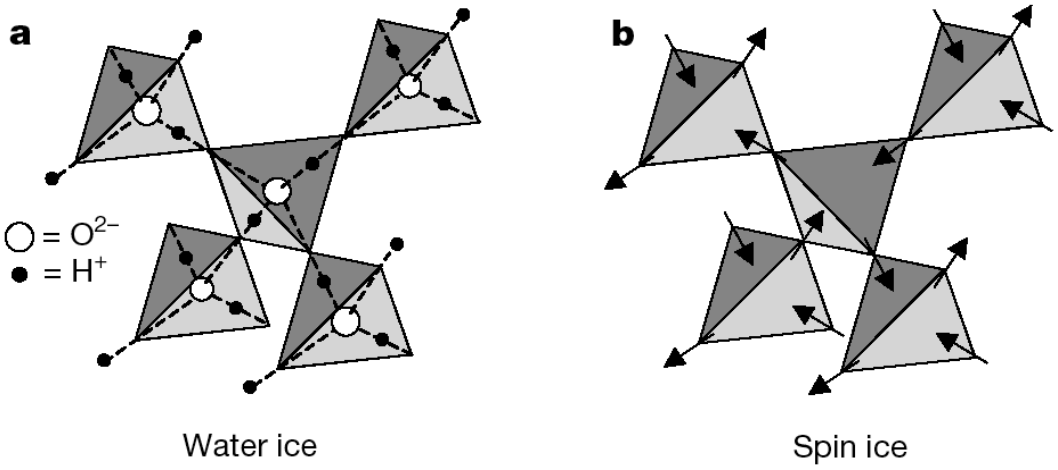

Figure 1.5: (a) proton arrangement in the frustrated water ice corroborates with the (b) spin arrangement in the frustrated spin ice compounds. [22]

1.4.1 Dipolar spin ice model

Initially, on the basis of positive Curie-Weiss temperature, a simple model of nearest-neighbor ferromagnetic interaction has been proposed to be responsible for the spin ice state in HTO and DTO [39], [44]–[46]. Later, Sidharthan et al. [47], pointed out the role of dipole-dipole interaction in rare earth titanate oxides ($R_2Ti_2O_7$). It has been suggested that the nearest-neighbor exchange interaction between rare earth Ising spins are purely antiferromagnetic, having a tendency to form a long-range ordered ground state. However, due to large magnetic moment (~$10\mu_B$) of Dy^{3+} and Ho^{3+} ions ferromagnetic dipolar interaction dominates over the antiferromagnetic exchange interaction. The strength of magnetostatic dipole-dipole interaction $D_{nn} = \mu_0\mu^2/(4\pi r_{nn}^3)$ is ~1.4 K, where (r_{nn}) is nearest–neighbor distance. Later, in 2000, den Hertog and Gingras [48] using numerical and mean field analysis shows that spin ice phenomenology in pyrochlores is purely associated with long-range dipole-dipole interactions. The proposed so-called dipolar spin ice model consists

of nearest neighbor exchange (first term) and long-range magnetic dipole interactions (second term) in the Hamiltonian is given as-

$$H = -J \sum_{<ij>} S_i^{\hat{Z}_i} . S_j^{\hat{Z}_j} + D r_{nn}^3 \sum_{i>j} \frac{S_i^{\hat{Z}_i} . S_j^{\hat{Z}_j}}{|r_{ij}|^3} - \frac{3\left(S_i^{\hat{Z}_i} . r_{ij}\right)\left(S_j^{\hat{Z}_j} . r_{ij}\right)}{|r_{ij}|^5} \qquad (1.2)$$

Where, J and D represent the exchange interaction and dipole-dipole coupling, respectively acting between spin vectors $S_i^{\hat{Z}_i}$ and $S_j^{\hat{Z}_j}$ situated at lattice sites i and j having orientation towards the local Ising <111> axis $\hat{Z}_i$. The $|r_{ij}|$ represents the distance measured in the units of the nearest-neighbor distance, r_{nn}. Through the use of Ewald summation techniques and considering the interplay of exchange and dipolar interactions, they proposed the phase diagram for pyrochlore magnetic system having Ising spins as shown in figure 1.6. Monte Carlo results show that spin ice behavior persists up to $J_{nn}/D_{nn} \sim -0.91$, where J_{nn} and D_{nn} are the nearest-neighbor exchange and dipolar interactions, respectively. For $J_{nn}/D_{nn} < -0.91$, a doubly degenerate second-order phase transition takes place in which all-in or all-out spin structure formed in the corner-shared tetrahedra. Furthermore, it has been found that in case of ferromagnetic exchange interaction, nearest-neighbor effective interaction $J_{eff} = J_{nn} + D_{nn}$ suppress the long-range effect of dipolar interaction and qualitatively nearest-neighbor spin ice physics came in the picture [39], [49]. In case of HTO and DTO, due to antiferromagnetic nature of the nearest-neighbor exchange, long-range dipolar interaction dominated over the nearest-neighbor effective interaction, J_{eff} one observes the broad feature in the specific heat showing the complex behavior of these compounds. In 2001, Bramwell et al. [50], confirms the proposed dipolar spin ice model through diffuse magnetic neutron scattering performed on HTO.

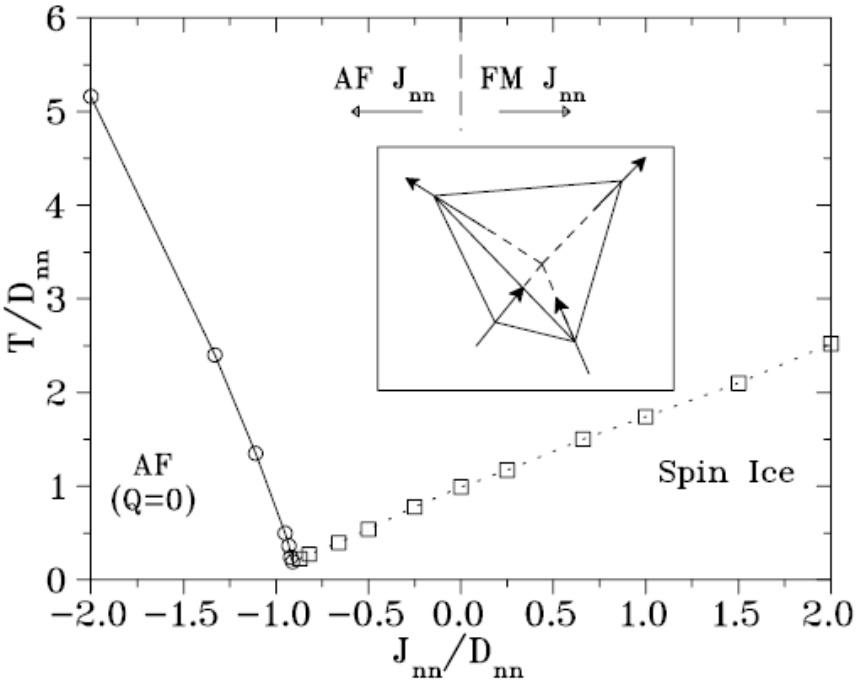

Figure 1.6: den Hertog and Gingras proposed phase diagram of pyrochlore magnets having Ising spin with nearest neighbor exchange and long rang dipolar interactions. J_{nn} and D_{nn} represent the Ising variables for nearest-neighbor exchange and dipolar energies. [48]

1.5 Crystal structure and single ion anisotropy

The crystal structure of DTO and HTO belongs to the face-centered cubic symmetry of space group $Fd\bar{3}m$, where Dy^{3+}/Ho^{3+} cation is situated at 16d site whereas Ti cation is situated at the 16c site of the crystallographic axis. Figure 1.7 shows the complex crystal structure of cubic pyrochlore oxides having space group $Fd\bar{3}m$.

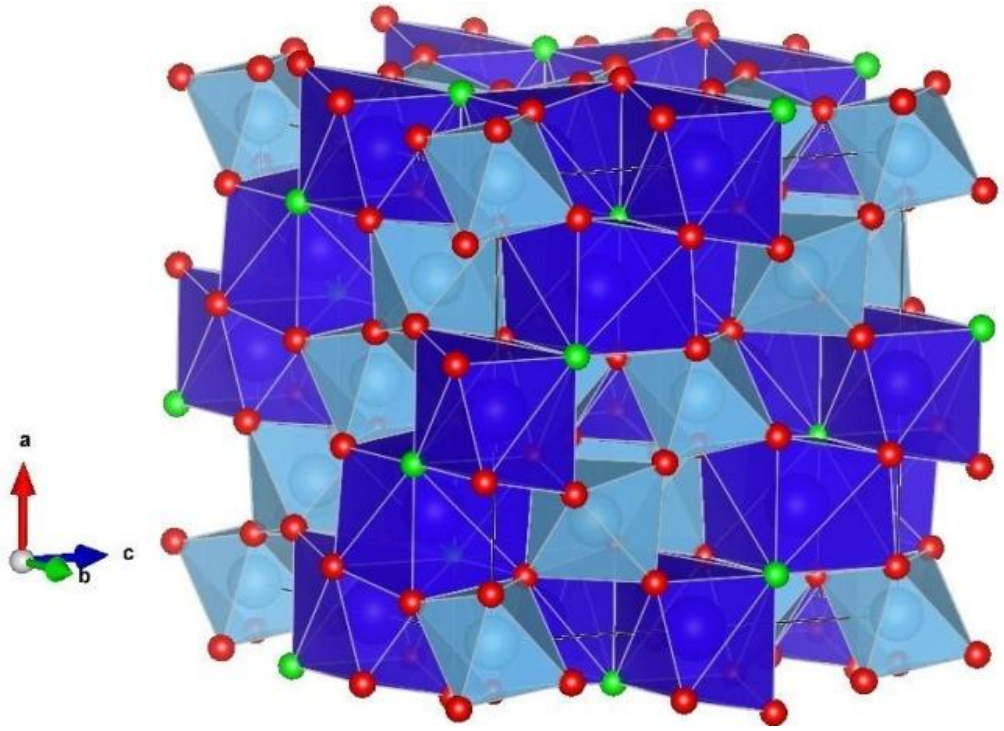

Figure 1.7: Complex crystal structural of cubic $R_2Ti_2O_7$ pyrochlore oxide having space group $Fd\bar{3}m$.

In the pyrochlore lattice, the oxygen environment around both cationic sites is quite interesting. The Ti ion is located in octahedral voids of $Fd\bar{3}m$ structure, whereas Dy^{3+}/Ho^{3+} ion is surrounded by eight oxygen ions. On the basis of oxygen position around Dy^{3+}/Ho^{3+} ion, one can categorize the oxygen ion position in two subclasses: the O1 sites (48f-site) represented by red colour and O2 sites (8b-site) represented as green colour in figure 1.8. The O1 oxygen is displaced in two parallel planar equilateral triangles arranged in an antiprismatic manner around the central Dy^{3+}/Ho^{3+} ion. This antiprismatic arrangement of O1 oxygen gives the D_{3d} point group symmetry which facilitates large distortion from the ideal cubic structure.

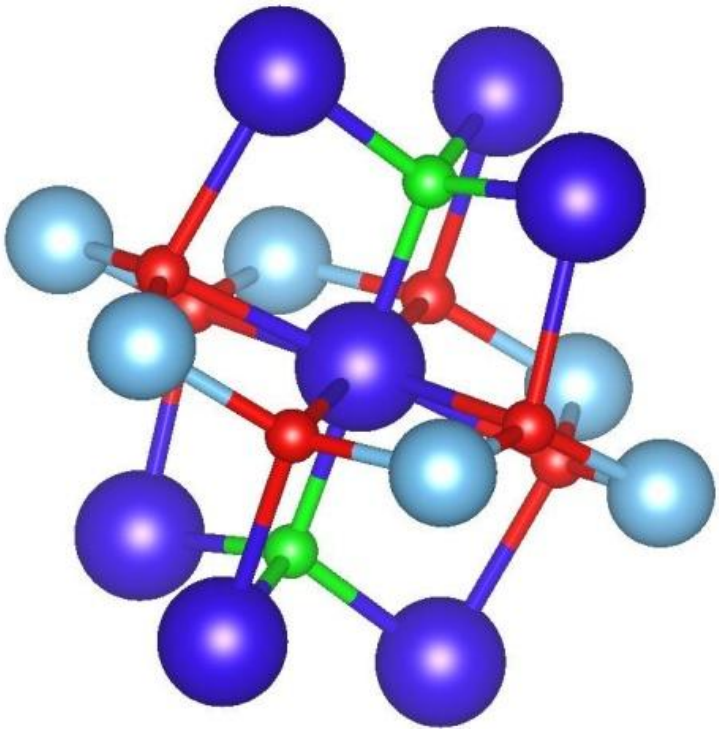

Figure 1.8: A part of pyrochlore structure of the $R_2Ti_2O_7$ cubic oxides (R = Ho/Dy) highlighting the oxygen environment around Rare Earth ion (blue color) and Ti^{4+} ion (sky blue color) formed by O1 (red color) and O2 (green color) oxygen sites.

The oxygen distortion from the ideal cubic structure is defined by the value of x in the 48f site. For the pyrochlore structure, x usually lies in the range 0.320 - 0.345, whereas x= 0.3125 for perfect octahedron around the 16c site [17]. The remaining two oxygen ions, termed as O2, are linearly aligned above and below Dy^{3+}/Ho^{3+} ion along local <111> axis of $Fd\bar{3}m$ space group as shown in figure 1.8. The distance between the Dy^{3+}/Ho^{3+} and O2 is ~2.2 Å, the shortest one known for any rare earth ion compound. This produces a strong axial anisotropy along local <111> crystallographic axis [23], [51], [52]. The Hamiltonian of the crystal field anisotropy is represented as-

$$H_{cf} = -D_{cf}\Sigma_I \langle S_i.z_i \rangle^2 \qquad (1.3)$$

Where, D_{cf} is crystal field anisotropy constant acting along z_i direction. This crystal field anisotropy split the 16 fold degenerate $^6H_{15/2}$ and 17 fold degenerate $^5I_8$ free ion ground state of Dy^{3+} and Ho^{3+} ions into multiple singlet and doublet states. In crystal field calculation study it has been found that the $^6H_{15/2}$ and $^5I_8$ ground state of Dy^{3+} and Ho^{3+} ions in DTO and HTO are separated from the first excited state are ~100 cm^{-1} (~150 K) and ~150 cm^{-1} (~215 K), respectively [52]–[54]. Such a large energy difference between the ground state and first excited state are also revealed from neutron scattering studies [55]. This pronounced crystal field anisotropy constrained the Ho^{3+} and Dy^{3+} ion's magnetic moment in such a way that it's maximum magnitude and direction lies along the local <111> axis of $Fd\bar{3}m$ crystal structure making the magnetic moment as Ising spin. In the pyrochlore lattice, these Ising spins of Ho^{3+} and Dy^{3+} ion are pointed out towards the center of the corner shared tetrahedra, preventing the long-range magnetic ordering in spite of effective ferromagnetic interactions in these compounds.

1.6 Static and dynamic magnetic properties of $Ho_2Ti_2O_7$ and $Dy_2Ti_2O_7$

1.6.1 Temperature dependent magnetization

In 2000, Bramwell et al. [56], studied the low temperature magnetization of HTO and DTO. As found previously in DC magnetization these compounds do not show any magnetic ordering in the temperature dependent magnetization. At lower temperature, both compounds show a monotonic increment without any spin freezing/transition. Analysis of temperature dependent low field susceptibility curve shows the weak ferromagnetic coupling between the magnetic rare earth spin having Curie Weiss temperature (Θ_{CW}) ~2 K and ~1 K for HTO and DTO, respectively as shown in figure 1.9.

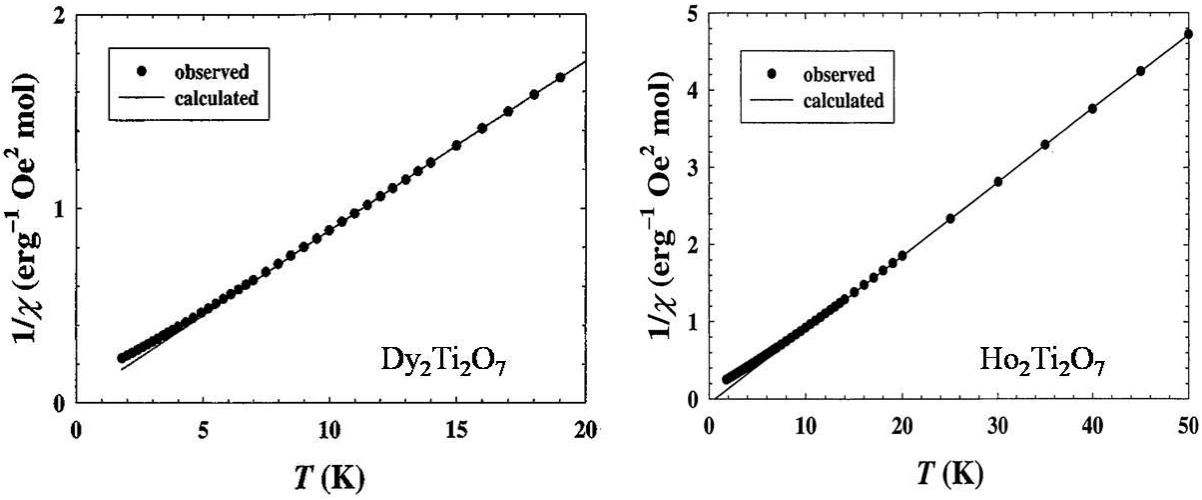

Figure 1.9: Temperature dependence of the magnetic dc susceptibility of $Dy_2Ti_2O_7$ (left) and $Ho_2Ti_2O_7$ (right). [56]

1.6.2 Magnetization vs. Magnetic field

To further investigate the magnetic behavior of HTO and DTO Bramwell et al. [56], measure the magnetic field dependent magnetization (M-H) in 0-7 T field range at different temperature as shown in figure 1.10. At a temperature 1.8 K M-H measurement of both compounds show the soft ferromagnetic nature in which a non-monotonic increment in the magnetization with the increasing magnetic field up to ~0.5 T takes place. On further increase in the magnetic field strength, magnetization gets saturated. On increasing temperature, M-H behavior changes from soft ferromagnetic to paramagnetic like thus suggesting the weakening of effective ferromagnetic dipolar interaction at higher temperatures. To measure the effective spin of HTO and DTO M-H data has been fitted by using two state powder-averaged theoretical equations and represented as solid line of figure 1.10. The good agreement between experimental and fitted data confirming the Ising nature

of Ho^{3+} and Dy^{3+} spin having magnetic moment m_J, ±8 and ±15/2 respectively for HTO and DTO as obtained from the effective value of Landé g-factor.

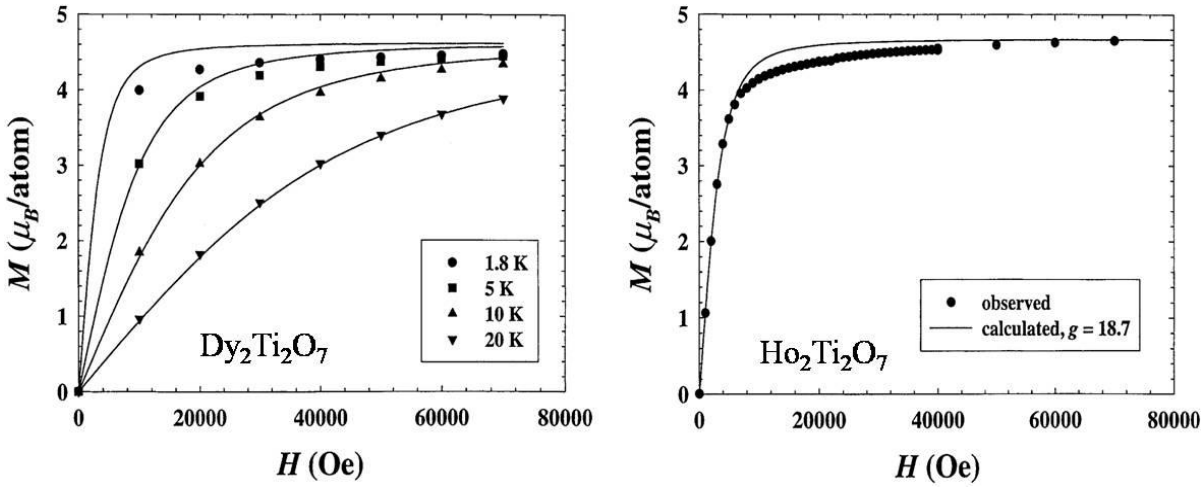

Figure 1.10: Magnetic field dependence of magnetization of $Dy_2Ti_2O_7$ (left) and $Ho_2Ti_2O_7$ (right). [56]

Later, in 2002, Matsuhira et al. [57], performed the M-H measurement on the single crystal of DTO along <111> crystallographic direction at a very low temperature. Their magnetic field dependent magnetization results are shown as figure 1.11. At temperature 0.48 K, they found two clearly distinguishable plateaus in the measured field range. On increasing temperature the intermediate plateau gets suppresses and only one plateau are observed. This observation was further confirmed by Matthews et al. [58]. Their studies concluded that along <111> crystallographic direction, pyrochlore lattice consists of alternate stacking of triangular and kagome lattice. On the application of magnetic field, spin ice state is persisted only up to 0.25 T. Whereas, in 0.25-0.75 T intermediate field range spins form kagome spin ice state in which triangular layered spin get aligned along the acting <111> magnetic field direction leaving kagome layer to remain disordered. On further increasing the magnetic field

strength disordered kagome layered spin ice state has been broken and form a stable 3in-1out or 1in-3out spin state in each corner shared tetrahedra. Figure 1.12 shows the formation of different spin arrangement on application of magnetic field along <111> crystallographic direction in stacked triangular and kagome plane of DTO.

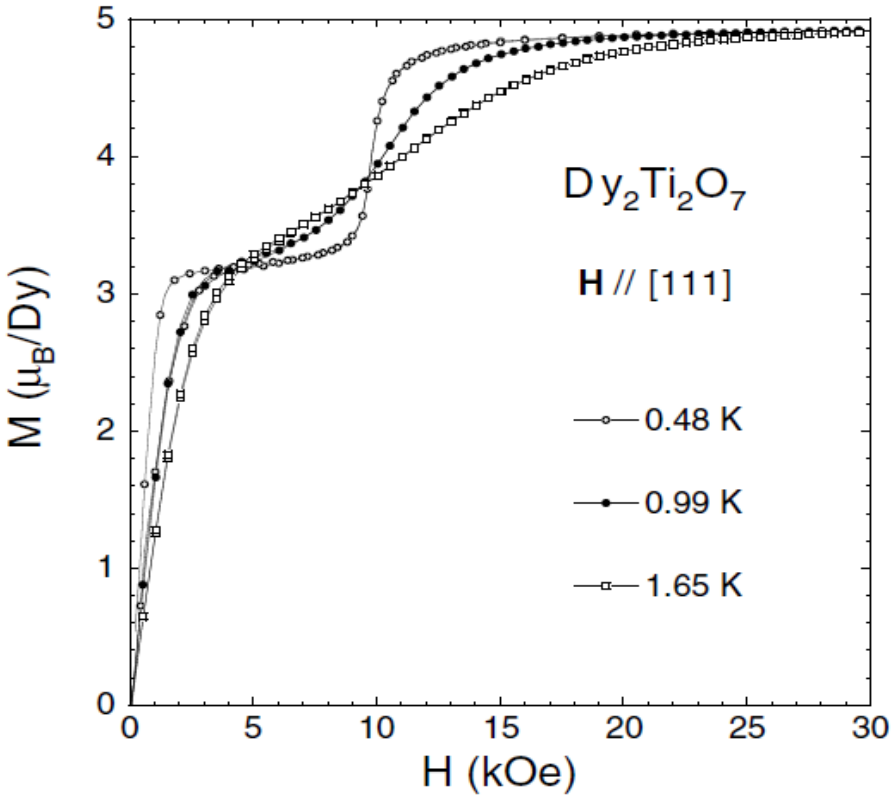

Figure 1.11: Field dependent magnetization of $Dy_2Ti_2O_7$ at different temperatures along <111> crystallographic direction. [57]

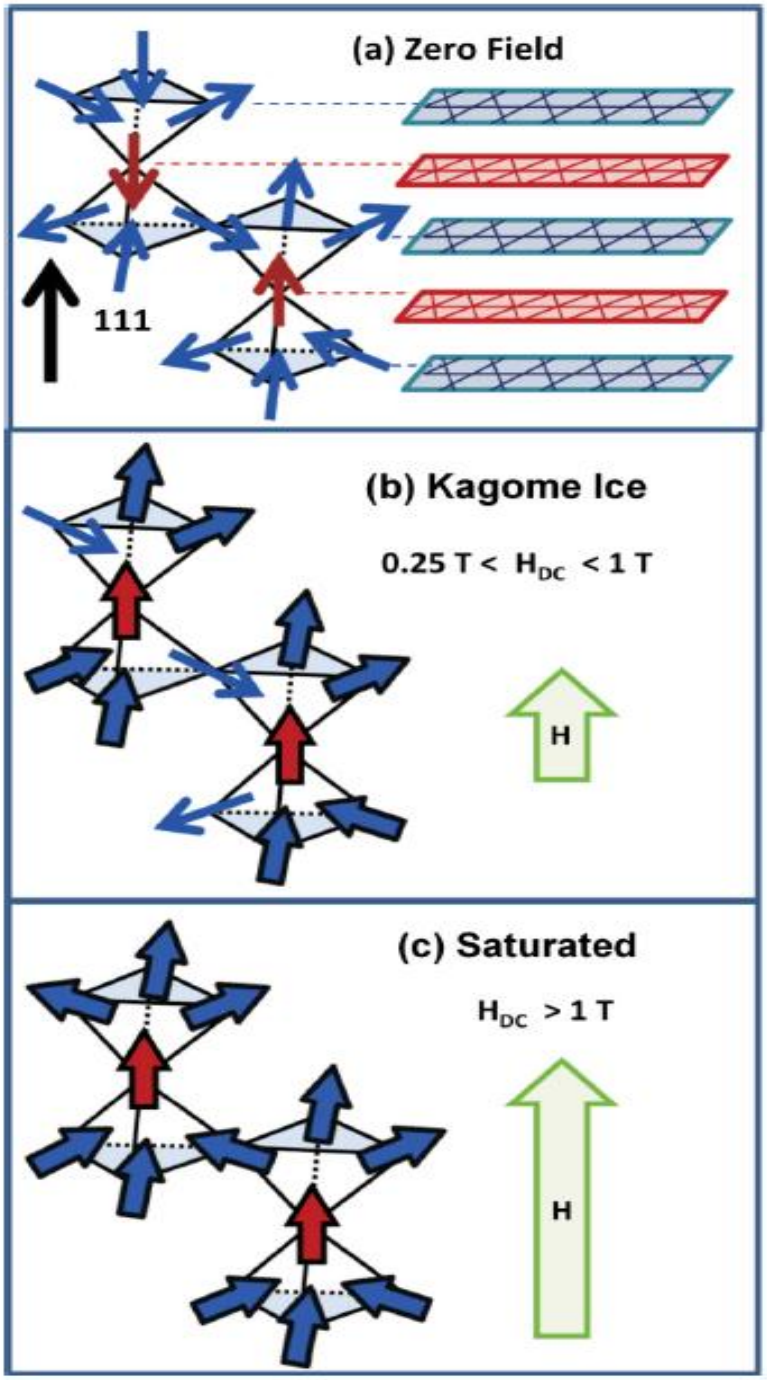

Figure 1.12: Formation of different magnetic state on application of magnetic field along <111> crystallographic direction in single crystal $Dy_2Ti_2O_7$. [58]

1.6.3 Dynamic properties of $Ho_2Ti_2O_7$ and $Dy_2Ti_2O_7$

The characteristics of the spin ice ground state in HTO and DTO have drawn tremendous interest for more than a decade. In these frustrated compounds, calorimetric study suggests that spin freezes into non-equilibrium magnetic state. [22] This drew attention to investigate the nature of spin dynamics in these compounds. Due to slower spin dynamics of, extensive magnetic ac susceptibility studies have been performed on DTO in comparison to HTO. Whereas, due to large neutron absorption of Dy in DTO, neutron scattering studies are mainly performed on HTO. Here, we present the literature review of the dynamic properties of DTO and their doped derivatives, and dynamic properties of HTO have been discussed later in section 1.6.3.3.

1.6.3.1 Dynamic properties of $Dy_2Ti_2O_7$

In 2001, Snyder et al. [41] studied the real (χ') and imaginary (χ'') parts of ac susceptibility of polycrystalline DTO. Figure 1.13 shows the temperature dependent ac susceptibility of polycrystalline DTO measured at different frequency. At lower frequency χ' (T) is virtually identical with χ_{dc}. Whereas, at higher frequency χ' (T) shows a sharp decrease at ~16 K with a simultaneous sharp rise in χ'' (T). On further decrease in temperature, a small increment in both χ' (T) and χ'' (T) takes place up to ~4 K, where a second spin freezing has emerged. Their study mainly focused on the nature of 16 K spin freezing whereas on the basis of previous low temperature specific heat and muon spin resonance study it has been suggested that 4 K spin freezing is associated with the formation of spin ice correlations [22], [39].

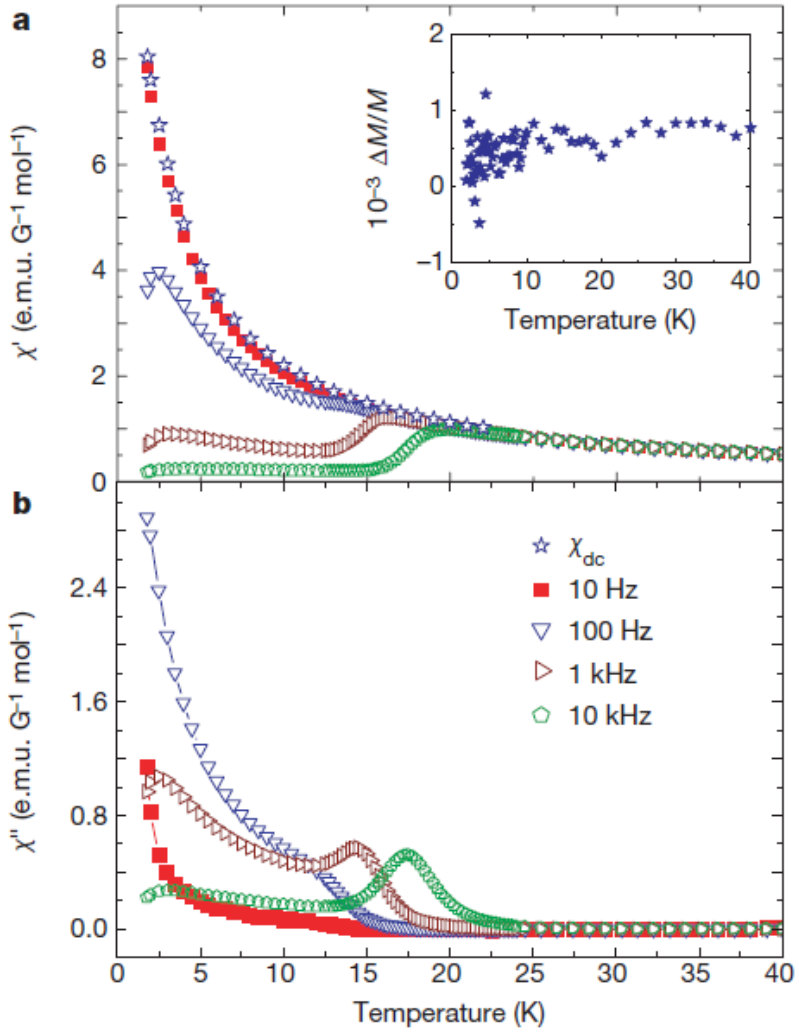

Figure 1.13: Temperature dependent ac susceptibility of $Dy_2Ti_2O_7$ at different frequency. [41].

The appearance and shifting of 16 K spin freezing (T_f) towards higher temperature with increasing frequency give the typical feature of spin glass behavior. However, the emergence of spin glass freezing in structurally and chemically ordered DTO is quite unusual. Frequency dispersion analysis of these spin freezing show the strong frequency dependent thermally activated behavior of T_f. The order of activation energy (~240 K) which is the order of crystal field anisotropy and narrow distribution of relaxation time suggest the single

ion like nature of T_f. The temperature dependent ac susceptibility performed in presence of different magnetic field of DTO, as shown in figure 1.14, shows that applied magnetic field enhances the magnitude of spin freezing and shift T_f towards the higher temperature side with increase in the magnetic field strength. In normal spin glass freezing, T_f gets suppressed by the external magnetic field and shifts towards the lower temperature side. This unusual behavior of T_f shows the exotic nature of spin freezing observed in DTO.

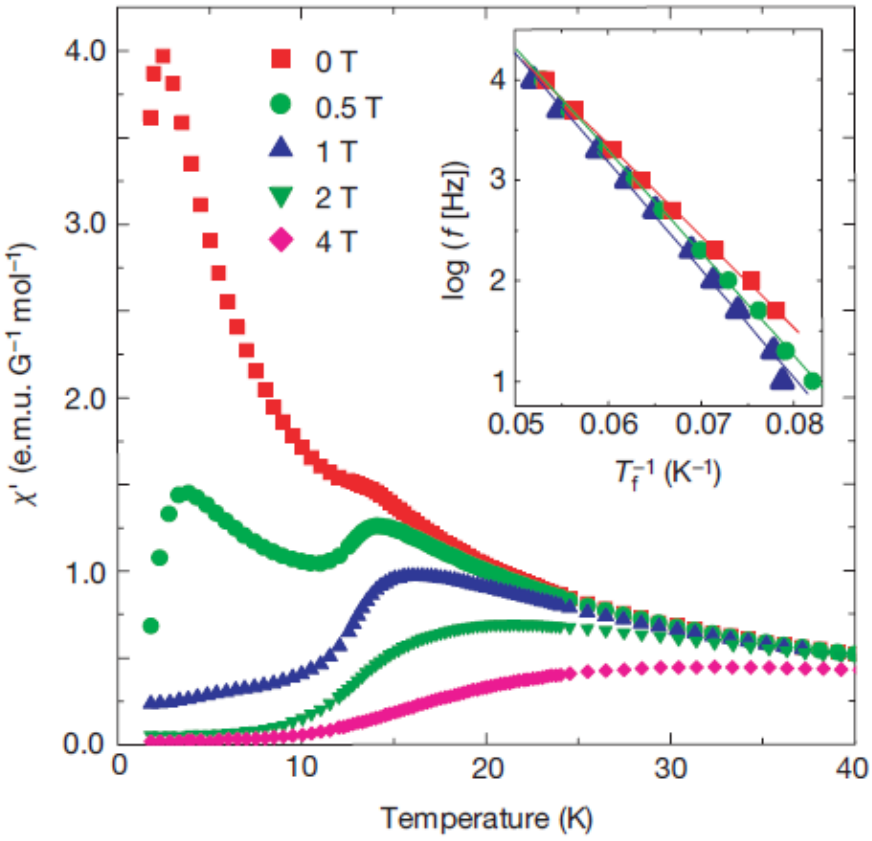

Figure 1.14: Temperature dependent real part (χ') of ac susceptibility of $Dy_2Ti_2O_7$ measured at different DC biased magnetic field. [41]

To understand the nature of spin dynamics in low temperature spin ice region, Matsuhira et al. (2001) [59], measured the AC susceptibly of DTO below 2.4 K. Figure 1.15 represents the temperature dependent normalized AC susceptibly of $Dy_2Ti_2O_7$ measured below 2.4 K. As one can clearly see in figure 1.15 spin ice freezing appears in χ' and χ'' at lower frequency (10 Hz) in contrast to higher frequency as observed for 16 K spin freezing. However, similar to 16 K spin freezing, spin ice freezing shows the frequency dependence of peak temperature. These observations show a slower relaxation process in lower temperature spin ice state.

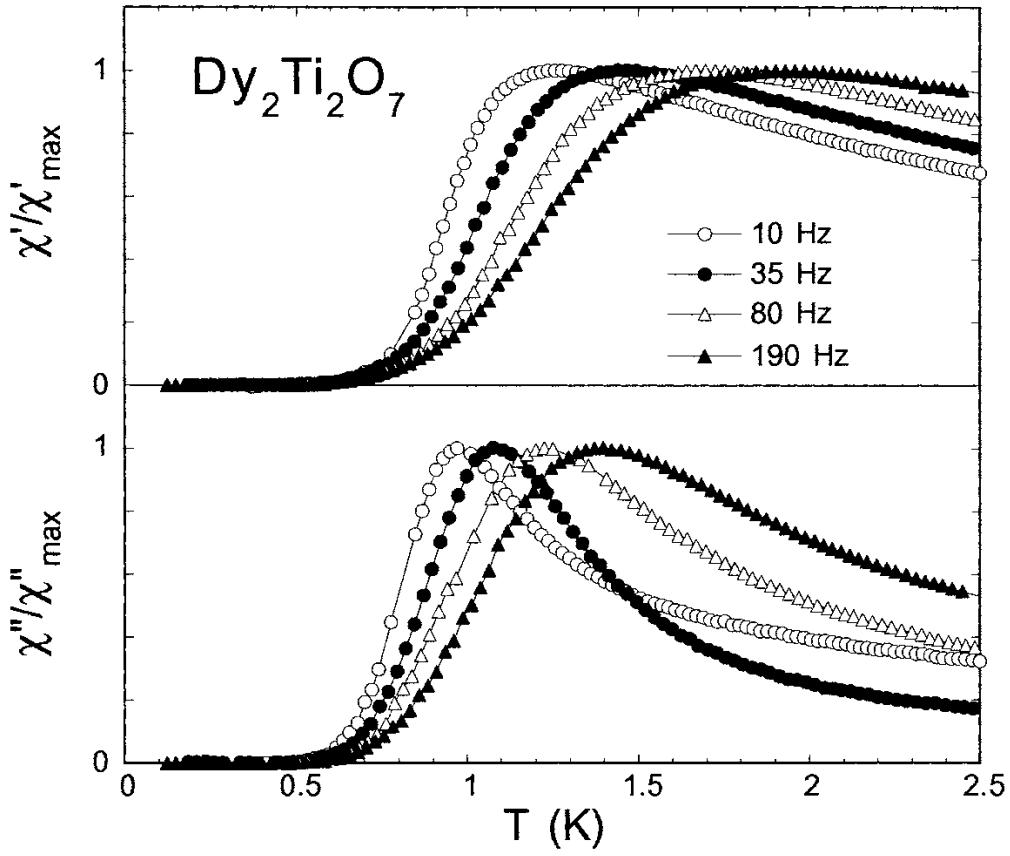

Figure 1.15: Normalized temperature dependent real (χ') and imaginary (χ'') part of ac susceptibility of $Dy_2Ti_2O_7$. [59]

To investigate the nature of spin dynamics they perform frequency dependence variation of the peak maxima of χ" for lower (T_m^L) and higher (T_m^H) spin freezing temperatures and temperature dependence of mean frequency obtained from the peak maxima of χ" from frequency dependent ac susceptibility plot. These findings are shown in figure 1.16**.** Frequency dependence inverse of T_m^L and T_m^H plot follows the Arrhenius behavior having activation energy of 220 K and 10 K, respectively. Their analysis concludes that below 10 K, spin relaxation is dominated by a slower relaxation process associated with ferromagnetic clusters having a tendency of short-range ordering due to the formation of spin ice configuration in each tetrahedra, whereas above 10 K spin relaxation is dominated by fast spin relaxations characterized by Davidson–Cole formula [60].

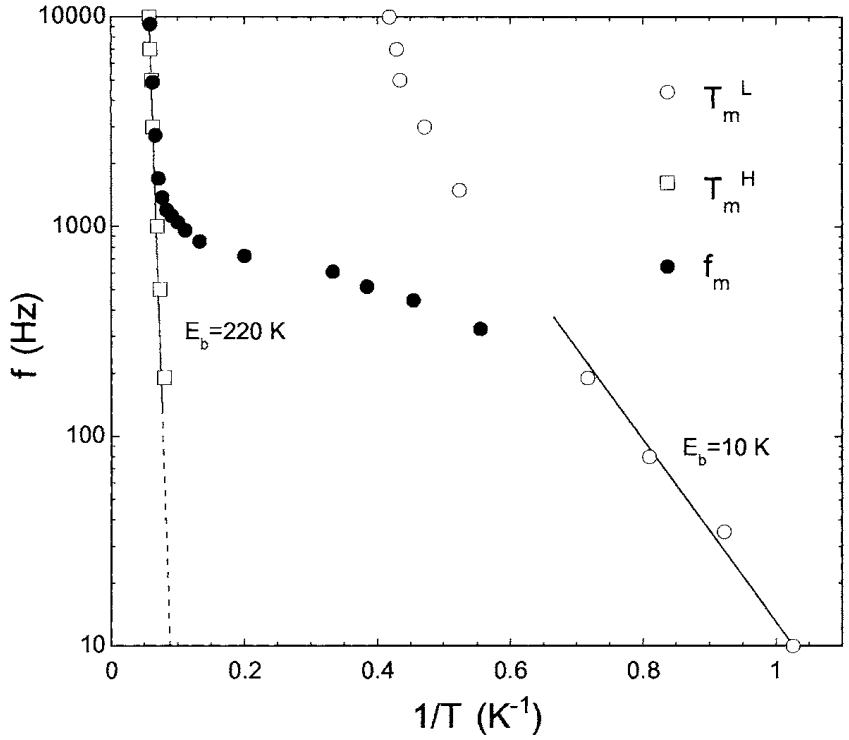

Figure 1.16: Plot of frequency dependence of inverse of $\boldsymbol{T_m^L}$ *and* $\boldsymbol{T_m^H}$ *and temperature dependence of mean frequency (*f_m*).* [59]

In (2003) Snyder et al. [61], investigated the temperature dependence of the spin relaxation time of DTO from frequency dependent χ'' measured at different temperatures. They performed these studies in the presence of different magnetic field as well and find that applied external magnetic field broaden the narrowly distributed relaxation time at lower temperature. Figure 1.17 shows the temperature dependence of the spin relaxation time of DTO at different magnetic field.

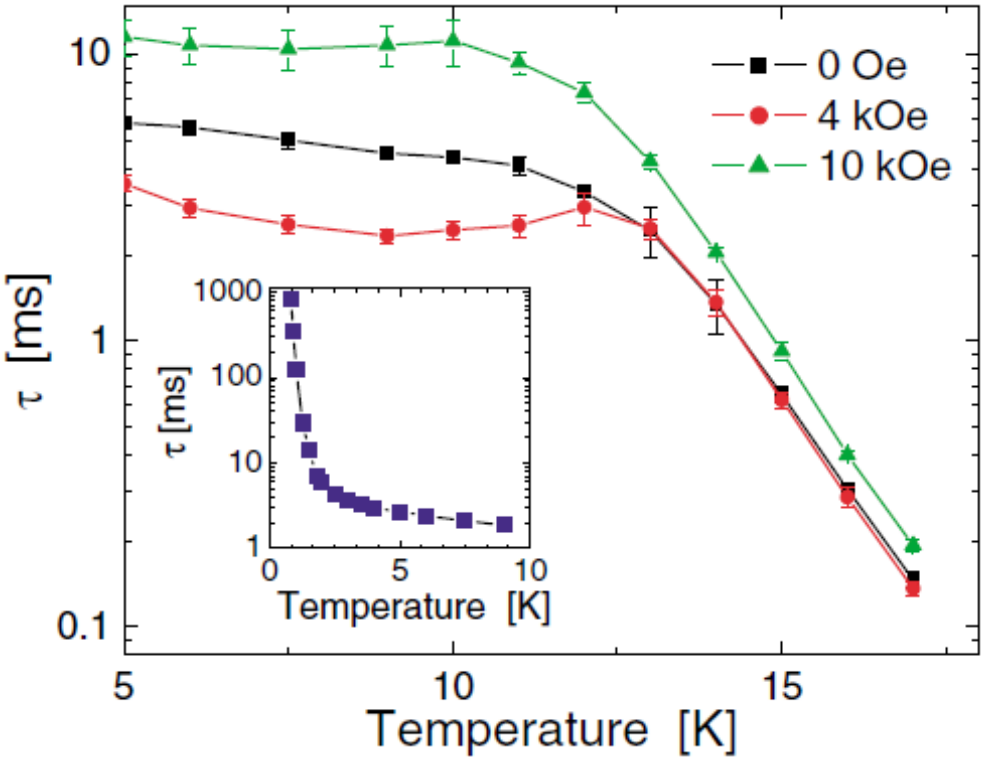

Figure 1.17: Temperature dependence of spin relaxation time of $Dy_2Ti_2O_7$ at different magnetic field. [61]

Temperature dependent relaxation time shows thermally activated behavior above ~13 K whereas below 13 K to ~4 K, it is almost temperature independent. Whereas below 4 K, a rapid increase in the relaxation time takes place, as shown in the inset of figure 1.17,

indicates the reemergence of thermally activated behavior at lower temperatures. They have concluded that up to ~13 K spin dynamics are governed by thermal fluctuations whereas below 13 K, it governed by temperature independent quantum fluctuation via quantum tunneling phenomena [62], [63]. The sharp increment in spin relaxation time below 4 K is possibly associated with the strong coupling of phonon with spin relaxation. To further investigate the nature of low temperature behavior of spin dynamics in 2004, Snyder et al. [64], measure the ac susceptibility of DTO at lower temperature. Their findings are shown in figure 1.18, which suggests that low temperature spin freezing follows the non-Arrhenius spin glass like behavior, showing the crucial role of quantum spin relaxation. It had been suggested that the reentrance of thermally activated nature of spin relaxation possibly associated with the development of spin-spin correlations.

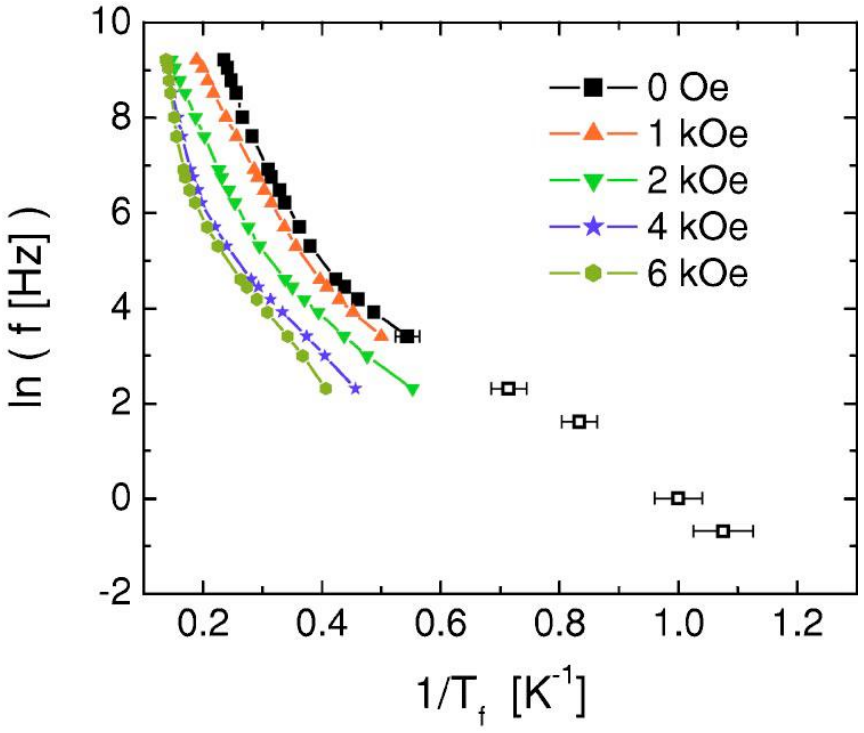

Figure 1.18: ln(f) vs. 1/T plot of $Dy_2Ti_2O_7$ at different magnetic field showing the non-Arrhenius behavior of spin relaxation. [64]

1.6.3.2 Effect of magnetic and non-magnetic dilution on spin freezing of $Dy_2Ti_2O_7$

Further, to investigate the nature and parameters which affect the both spin freezing observed in DTO, a number of magnetic and non-magnetic dilution studies have been performed. In 2004, Snyder et al. [65], study the effect of magnetic dilution by substituting the non-magnetic yttrium ion at Dy site on spin dynamics of $Dy_{2-x}Y_xTi_2O_7$ compound for x= 0-1.98 concentration range. Figure 1.19 shows the temperature dependent ac susceptibility measured foe different composition for $Dy_{2-x}Y_xTi_2O_7$ compound. ac susceptibility study shows the suppression in both the freezing up to a concentration of x= 0.4 suggesting the existence of local spin correlation involved in the 16 K spin freezing process. For higher concentration, spin freezing re-emerged and shifted towards the higher temperature side with increasing concentration. A similar observation has been found in case of non-magnetic Lu ion substitutions at the Dy site in DTO. These findings show the robust nature of 16 K spin freezing having single ion nature of the distribution of spin relaxation time. They have concluded that observed freezing is fundamentally a single spin process that is affected by the local environment, rather spin-spin correlations as they predicted in their previous studies [66]. It was quite surprising that low temperatures spin freezing also shows the robust nature and existed up to x= 0.8 of non-magnetic yttrium. Further, Liu et al. [67], suggest that crystal field-phonon coupling also contributes in the spin dynamics of single crystal $Dy_{2-x}Yb_xTi_2O_7$ which can be affected by the altered crystalline electric field and magnetic interactions. A similar kind of observation has been found by Ke et al. [68], in magnetothermal study of hybrid (spin liquid-spin ice) frustrated $Dy_{2-x}Tb_xTi_2O_7$ shown as figure 1.20. Their analysis shows that inclusion of Tb in $Dy_2Ti_2O_7$ strongly affects the thermal and magnetic properties suggesting the complex nature of spin dynamics. It has been noted that both spin freezing get

affected with increasing Tb concentration. Their observation concludes that low temperature magnetic behavior of DTO can be altered by alteration in crystalline electric field as well as Dy-Tb spin interaction.

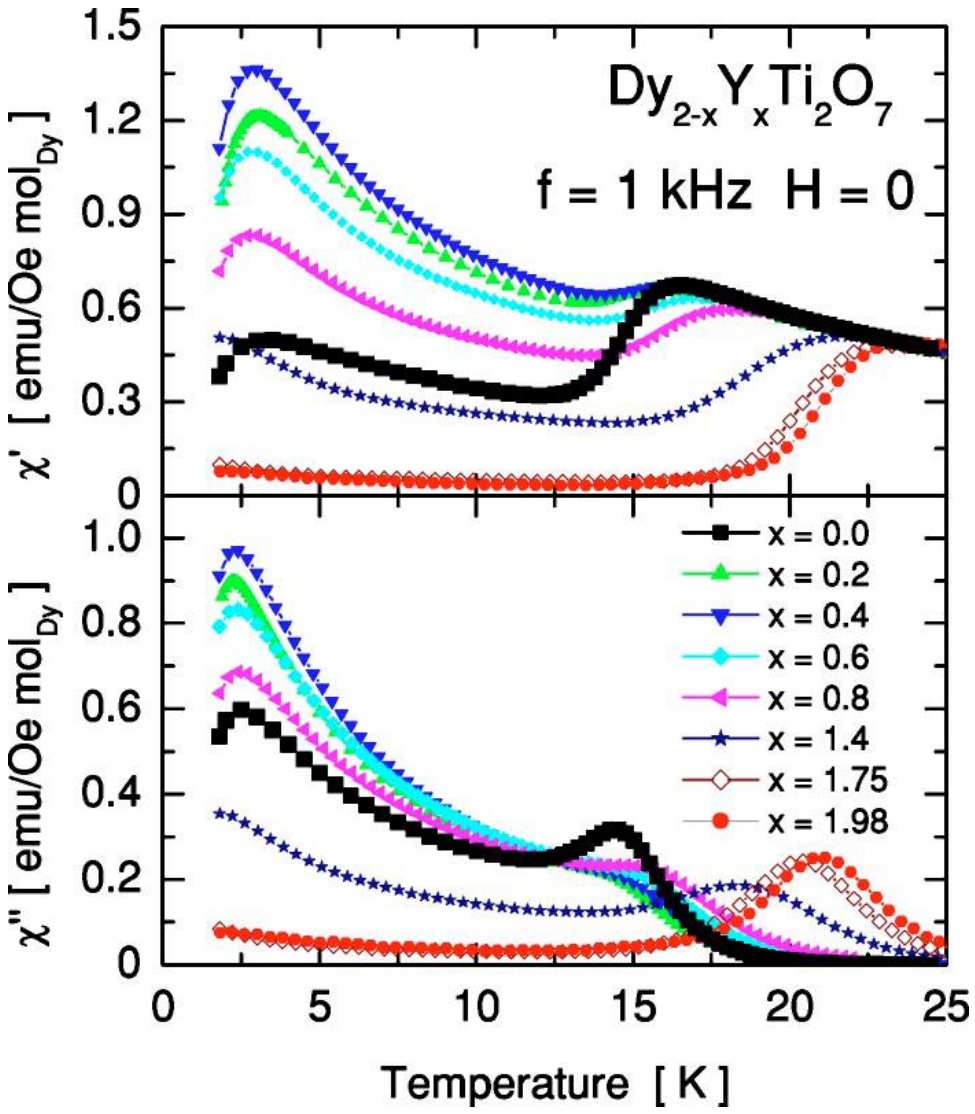

Figure 1.19: Temperature dependent ac susceptibility (χ' and χ'') of $Dy_{2-x}Y_xTi_2O_7$ measured at 1 kHz applied frequency. [65]

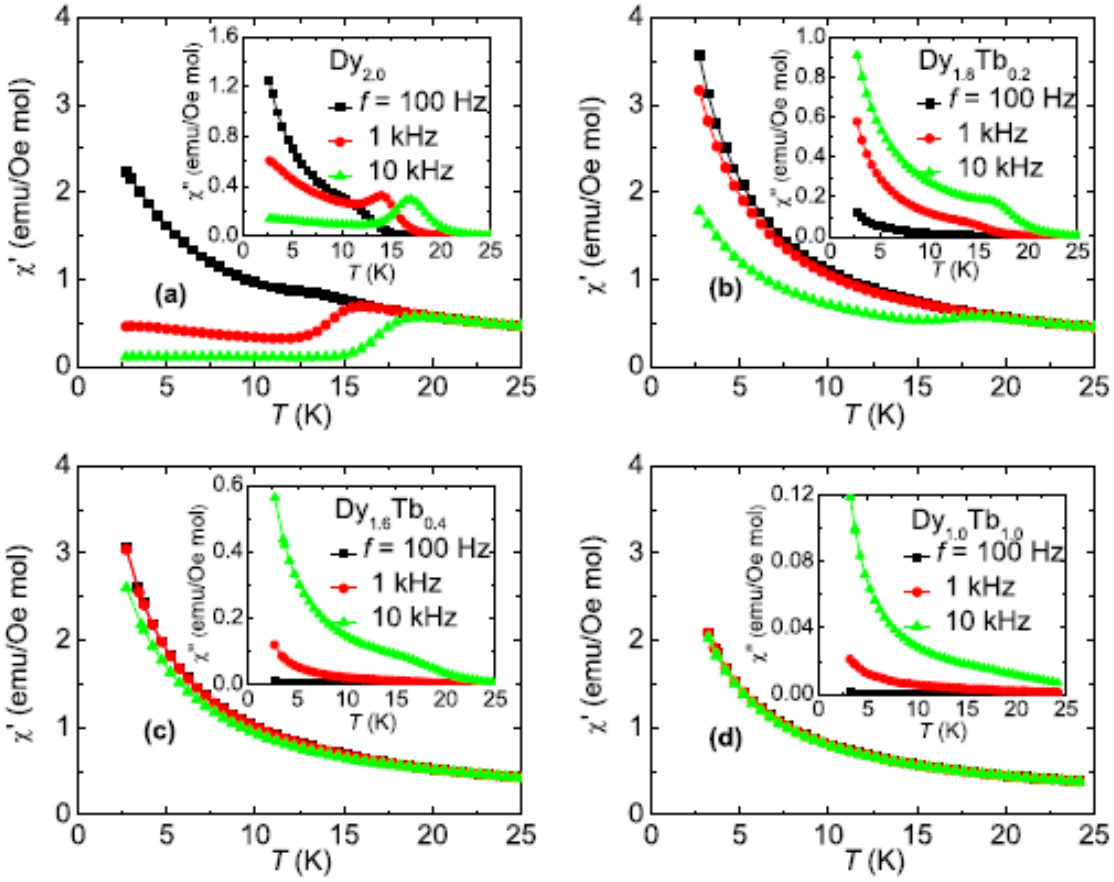

Figure 1.20: Temperature dependence of the real part (χ') of ac susceptibility of $Dy_{2-x}Tb_xTi_2O_7$ *at 1 kHz and 10 kHz frequency.* [68]

These studies show the complexity of spin dynamics in DTO which is affected by the alteration in the local crystal field environment, spin correlations, and magnetic interactions. However, these studies have been performed at higher substitution due to which real mechanism cannot be concluded decisively. The robustness of both spin freezing for magnetic and non-magnetic dilution indicates that in this compound spin dynamics do not get affected by the neighboring magnetic spin though existing long-range dipolar correlation at lower temperatures. Due to the presence of magnetic frustration, it is important to know the sensitive control variable which affects the spin dynamics of DTO. Out of local crystal field

distortion, spin correlation and spin-spin interaction, which process plays more significant role in the spin dynamics is a matter of investigation.

1.6.3.3 Dynamic properties of $Ho_2Ti_2O_7$

On the other hand, limited dynamic studies via ac susceptibility have been performed on HTO. Unlike DTO, in HTO only low temperature spin ice freezing has been observed in magnetic ac susceptibility measurements. The major ac susceptibility study was performed by Matsuhira and co-workers [42]. Figure 1.21 shows the temperature dependent ac susceptibility at different frequencies. In temperature dependent χ', a dramatic drop at ~1.2 K has been observed, which magnitude becomes approximately zero around 0.5 K. Additionally, a peak appeared at ~1.0 K in temperature dependent χ''. They noted that observed peak position in χ' and χ'' get shifted towards the higher temperature with increasing frequency thus showing a typical behavior of glassiness. The temperature dependence of peak position of observed spin freezing suggests the thermally activated behavior of spin in HTO at lower temperature. The analysis of frequency dispersion of the χ'' peak position shows the thermally activated Arrhenius behavior having activation energy 27.5 K.

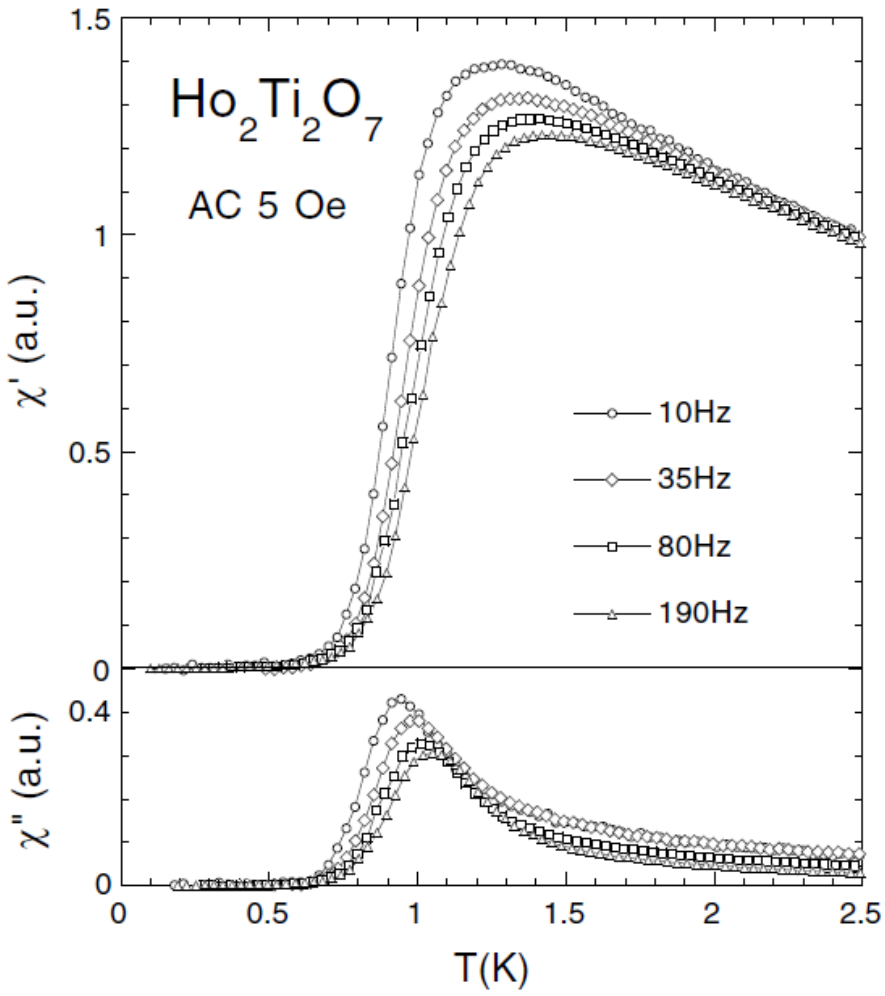

Figure 1.21: Temperature dependent ac susceptibility of $Ho_2Ti_2O_7$ measured at different frequency. [42]

Later, in 2003, Ehlers et al. [69], perform the neutron spin echo and ac-susceptibility study on HTO. Neutron spin echo reveals that similar to DTO in HTO as well two spin relaxation processes are involved and a peak at ~15 K should emerge in ac susceptibility. To investigate the 16 K spin freezing they performed the temperature dependent ac susceptibility at different magnetic field as shown in figure 1.22.

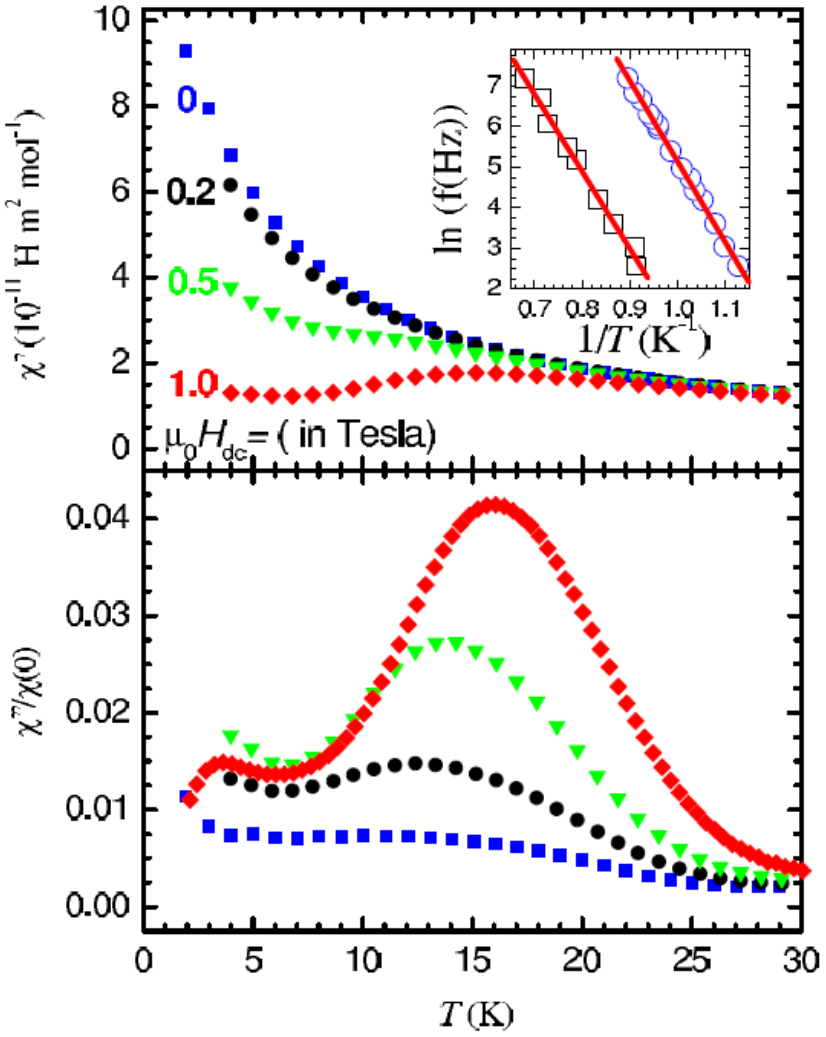

Figure 1.22: Appearance of spin ice and 16 K spin freezing in temperature dependent ac susceptibility of $Ho_2Ti_2O_7$ measured at different magnetic field. [69]

It has been noted that on the application of magnetic field, both low entropy spin ice and higher temperature spin freezing (T_f) appeared. However, at lower external magnetic field T_f freezing is observable but indistinguishable. It has been found that both spin freezing temperature strongly depends on the magnetic field strength. The appearance of both spin freezing in HTO showing the involvement of two distinct relaxation mechanisms at lower temperature similar to DTO. To reach clearer conclusion about the nature of magnetic field

induced T_f spin freezing, Ehlers et al. (2004) [70], reinvestigate the nature of low temperature spin dynamics of HTO via neutron and ac susceptibility study. From neutron scattering study they observed that in 2-30 K temperature range spin relaxation is temperature independent. Further, in ac susceptibly study measured in presence of different frequency as shown in figure 1.23.

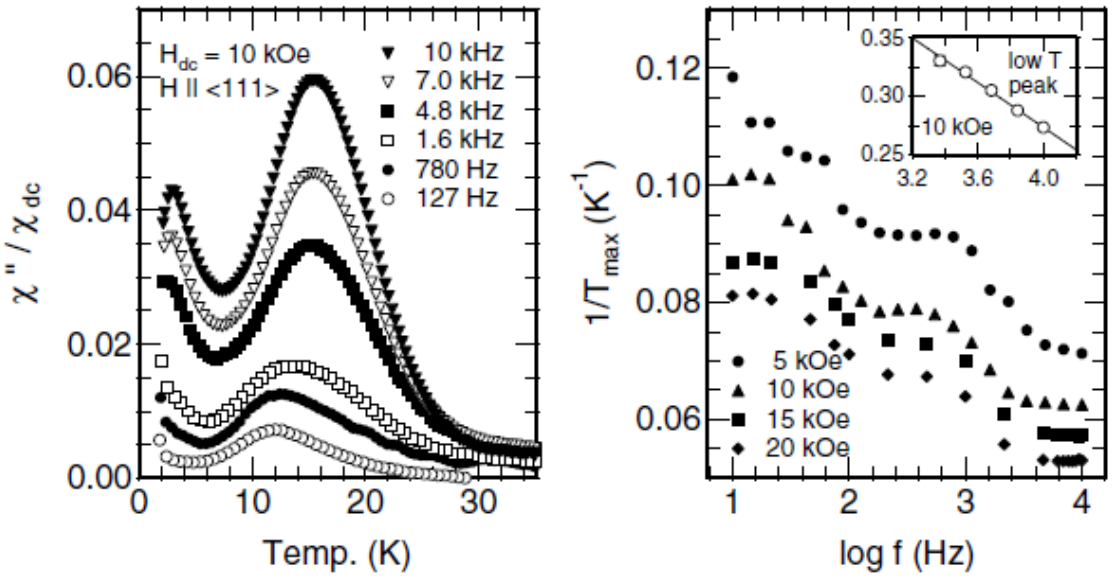

Figure 1.23: Temperature dependent ac susceptibility of single crystal $Ho_2Ti_2O_7$. Left panel: χ''/χ_{dc} measured at different frequency in presence of 1 T external magnetic field. Right panel: Variation in the inverse of high temperature spin freezing temperature (T_f) with ln(f) at different external magnetic field. Inset shows the variation in the inverse of spin ice freezing temperature with ln(f)at 1 T external magnetic field. [70]

In presence of 1 T external magnetic field, spin ice and higher temperature spin freezing appeared at ~4 K and ~15 K, respectively. It has been noted that both freezing temperatures shifted towards the higher temperature with increasing frequency thus showing the thermally activated behavior of spin dynamics in HTO. Frequency dispersion analysis shows the non-

Arrhenius nature of higher temperature spin freezing whereas low temperature spin ice freezing follows the Arrhenius behavior. However, frequency shift of low temperature spin ice freezing and higher temperature spin freezing shows the activation energy ~24 K (~2.07 meV) and ~250 K (~21.5 meV), respectively. Their analysis concluded that spin-flip process is single spin mediated by crystal field above 15 K. At low temperature (below 4 K) spin-flip process is governed by the quantum tunneling taking place in between the Ising doublet having some energy barrier. This process is slower than the higher temperature processes.

Later, in 2009, Clancy et al. [71], reinvestigate the static and dynamic magnetic properties of HTO through elastic and inelastic neutron scattering measurements. From diffuse neutron scattering studies, it has been demonstrated that at 10^{-9} sec (measurement time scale), spin ice ground state formed below 2 K is static in nature whereas above 2 K, spins retain a paramagnetic state. In paramagnetic state, a temperature independent relaxation rate has been observed in 3-30 K temperature range whereas above 30 K spin relaxation rate becomes temperature dependent. Figure 1.24 shows the temperature dependence of spin relaxation time of HTO obtained from neutron scattering studies. A similar finding has been observed by Ehlers et al. [72], in neutron scattering study performed on $Ho_{2+x}Ti_{2-x}O_{7-\delta}$ stuffed spin ice compounds. In these studies, it has been concluded that temperature independent region showing the spin relaxation mechanism is governed by the quantum fluctuation via quantum tunneling. Above 30 K, a quantum to classical crossover takes place where spin relaxation time is dependent of the thermal fluctuations.

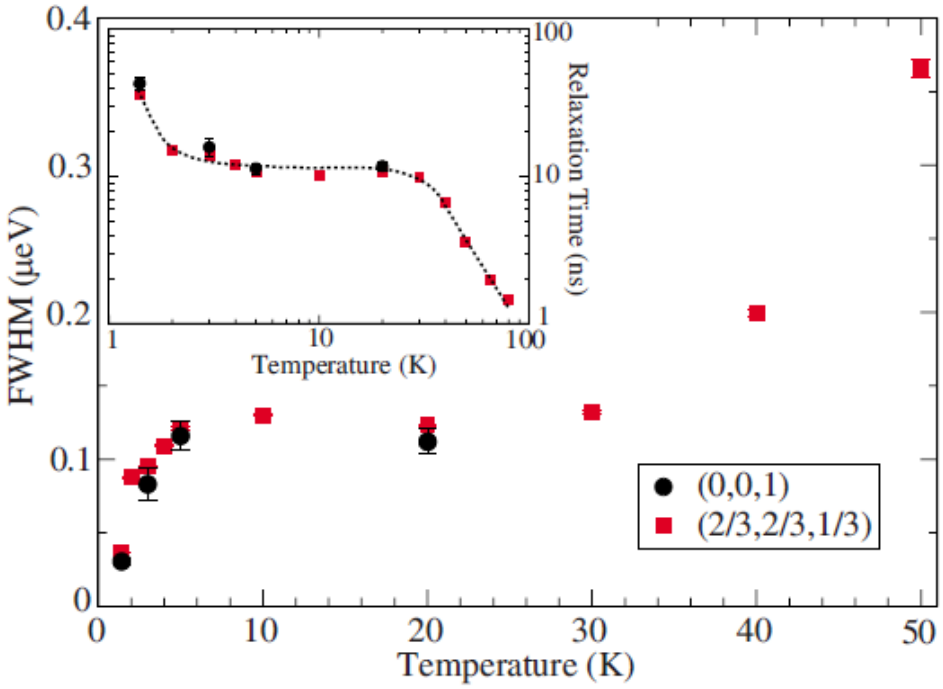

Figure 1.24: Temperature dependence of the FWHM of the quasielastic signal of neutron scattering of $Ho_2Ti_2O_7$. Provide the temperature dependent variation in the spin relaxation time shown in the inset. [71]

1.6.4 Quantum-classical correspondence in $Ho_2Ti_2O_7$ and $Dy_2Ti_2O_7$

These observations show that in HTO and DTO quantum fluctuation are dominated over 30 K and 13 K, respectively [61], [71], [72]. The region in which quantum fluctuation governs the spin dynamics are known as "quantum critical region". The thermal dependency of spin ice freezing and higher temperature T_f spin freezing shows the classical behavior. As it is known that on decreasing temperature thermally energy decreases and quantum fluctuations dominate over the thermal energy, which drives the spin dynamics. It is quite surprising that once, quantum fluctuation dominated over the thermal energy then how thermal energy again controls the spin dynamics in both compounds.

Further, existence of quantum critical region up to ~30 K in HTO and ~13 K in DTO indicates that both spin freezing temperature of these materials can be investigated in terms of "quantum criticality" of the Quantum Phase Transition. Though quantum fluctuations occur only at absolute zero temperature, known as quantum critical point (QCP), its remarkable impact can be observed in the region of 'quantum criticality' existing at a finite temperature, where quantum fluctuations dominated over the thermal fluctuations. The phase transitions taking place in the region of "quantum criticality" is known as quantum phase transition (QPT) [73]–[75]. In the quantum critical region, QPT follows the $(x\text{-}x_C)^{1/2}$ behavior with non-thermal parameters whereas in the classical region it follows $(x\text{-}x_C)$ type variation [76]–[78]. Through the application of non-thermal control variables, such as pressure (P), composition(x), or magnetic field (H), one can obtain the QCP as well as the region of quantum criticality of the materials. The magnetic field dependency of both spin freezing observed in HTO and DTO suggest the magnetic field is one of the control variables of spin dynamics to discriminate the quantum and classical region of these compounds.

The quantum mechanical behavior of spin dynamics brings these dense frustrated spin systems in the category of quantum materials. In quantum state of quantum materials, macroscopic properties are governed by ground state quantum fluctuations in which quantum information are propagated in a correlated manner with temporal evolution [79]–[81]. Due to quantum correlation, these quantum materials have memory to distinguish their widely differing initial conditions i.e. properties of these materials depending on initial conditions. At finite temperature, thermalization phenomena erase the memory of the quantum system by dephasing the quantum correlation [82]–[84] and put a limit for the experimental realization of quantum information. Recently, experimental realization of scrambled quantum

information in atomic and bi-particle quantum systems triggered a new hope to study the exotic quantum behavior of other quantum materials [79], [81], [82]. Experimental findings reveal that in these quantum systems, due to the ergodic nature of microstate, thermalization phenomena of each microstate occurs individually though they are strongly correlated with each other [82], [85], [86]. This means that dephasing of quantum correlations are taking place at the microscopic level and for the study of exotic quantum behavior in materials, prevention of thermalization is mandatory and remains a challenge. The unawareness of measurement protocol which set bound on thermalization to reach the system in thermal equilibrium and crucial variable of exotic quantum behavior further increases the puzzle. The emergence of classical behavior in the quantum critical region shows the thermalization of spin may be responsible for the classical nature of spin in the quantum critical region in these materials. However, the search of crucial variable which set bounds on the spin thermalization in these dense spin systems for the extraction of quantum correlation induced scrambled quantum information is a challenging task and a matter of investigation.

1.7 Ferroelectricity in $Ho_2Ti_2O_7$ and $Dy_2Ti_2O_7$

Along with these challenges of the complex magnetic behaviors, these cubic materials having space group $Fd\bar{3}m$ show multiple multiferroic transitions observed in different temperature regime [87]–[90]. First of all, in (2009), Dong et al. [87], dielectric and pyroelectric study reported the presence of two ferroelectric transitions in HTO. Figure 1.25 shows their temperature dependent dielectric permittivity of HTO measured at different frequency. In the measured temperature range two dielectric relaxations are observed at ~23 K and ~90 K, respectively with decreasing temperature. Shifting of relaxation temperature towards the higher temperature side with increasing frequency in dielectric permitivity ε (T) and loss

tangent tan(δ) showing the typical relaxation characteristic of relaxor ferroelectric. To further investigate the presence of ferroelectricity they performed the temperature dependent pyroelectric study as shown in figure 1.26. Pyroelectric study shows two anomalies at ~20 K and ~53 K, respectively suggesting the ferroelectricity in HTO. They have concluded that higher temperature 53 K ferroelectric transition is a relaxor ferroelectric transition associated with the structural distortions associated with the Ti site. Whereas, low temperature 20 K ferroelectric transition is related with complex magnetism of HTO.

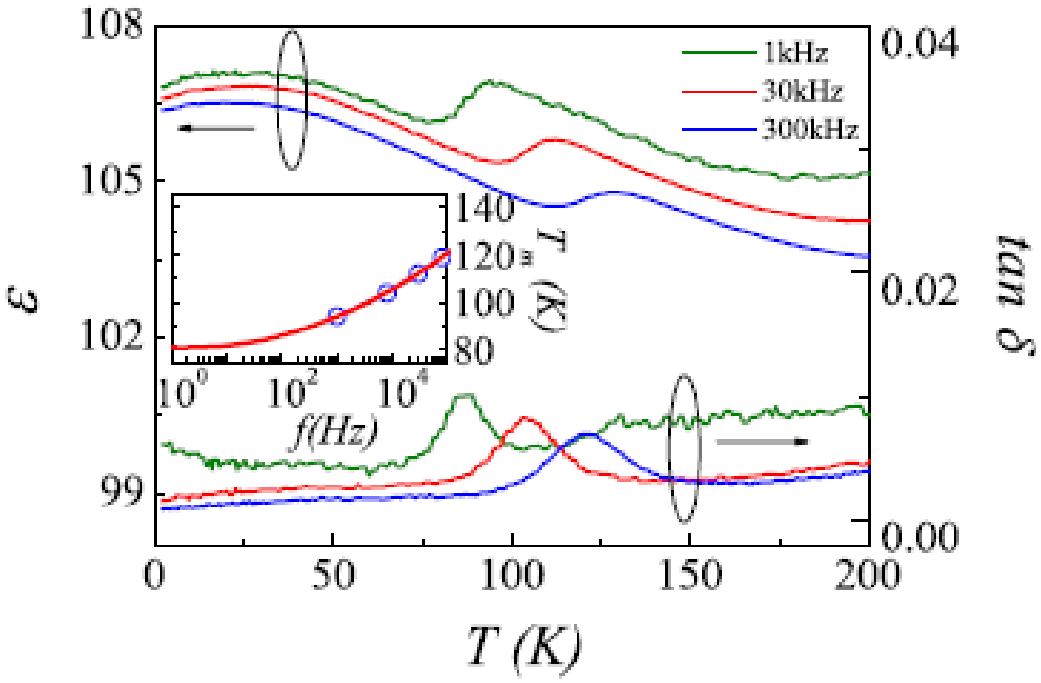

Figure 1.25: Temperature dependence of the dielectric permittivity (ε) and dielectric loss (tanδ) of $Ho_2Ti_2O_7$ measured at different frequency. [87]

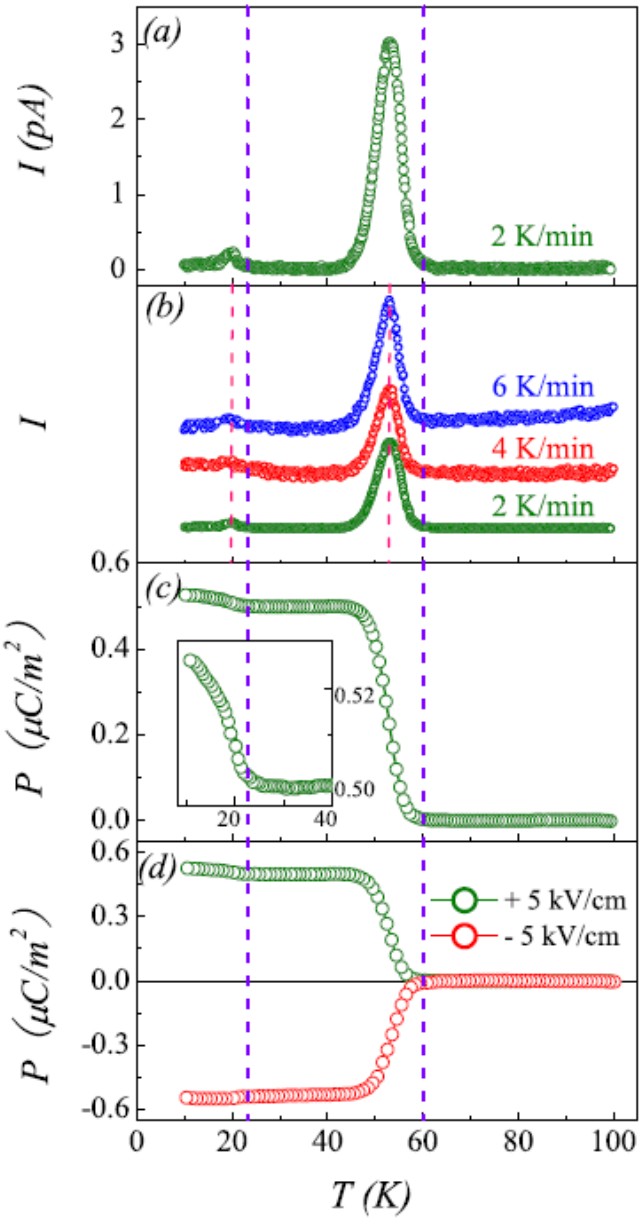

Figure 1.26: Temperature dependence of; (a) pyroelectric current (I), (b) under a series of warming rates, (c) polarization (P) and (d) polarization under a positive and negative poling electric field of $Ho_2Ti_2O_7$. [87]

To further understand the emergence of ferroelectricity, Dong et al. [91], perform the pyroelectric study on Cr doped $Ho_{2-x}Cr_xTi_2O_7$. On increasing Cr concentration an increment and enhancement in the ferroelectric transition temperature and ferroelectric polarization has

been observed. It has been concluded that Cr induced structural distortions and Dzyaloshinskii-Moriya interaction (DMI) are responsible for the enhancement in the ferroelectric transition temperature and polarization. A similar observation has been reported by Lin et al. [92], in the magnetic and pyroelectric study of Fe doped $Ho_{2-x}Fe_xTi_2O_7$. In the temperature dependent pyroelectric study they observed two ferroelectric phase transition at ~30 K and ~80 K, respectively. On Fe substitution, a large increment in the ferroelectric polarization has also been noted. In this study, it has been suggested that observed ferroelectric transitions have originated from complex magnetism of HTO. To understand the nature of ferroelectric transition Liu et al. [89] performed the pyroelectric study on single crystal of HTO along (110) and (111) orientation. In the I-T curve shows a broad peak at ~14 K along (110) orientated sample whereas a sharp peak plus the broad peak over the measured temperature range for (111) oriented sample. Through the field dependent polarization study they have concluded that observed transition is ferroelectric transition associated with magnetic 3in-1out spin structure. However, in (2004), Katsufuji et al. [93], perform the magnetocapacitance study on single crystal HTO along (100) and (111) direction, shown as figure 1.27, already reported the magnetism induced magnetocapacitance in HTO. It their findings, it has been found that on application of magnetic field a clear change in the dielectric constant has been taking place. This change becomes more pronounced with decreasing temperature. From the analysis of magnetic field dependent magnetization and magnetocapacitance, they have concluded that at low temperature magnetocapacitance is dominated by ferromagnetic or antiferromagnetic fluctuations. In these findings, multiple ferroelectric transitions in HTO at different temperatures of structural and complex magnetic origin have been proposed.

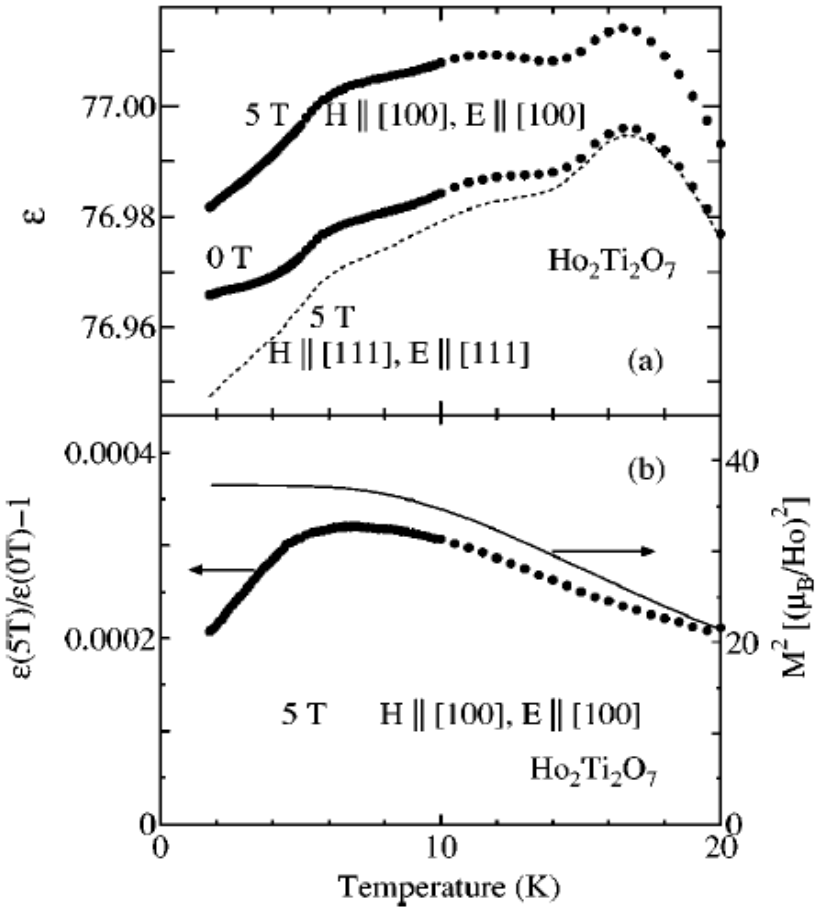

Figure 1.27: (a) Temperature dependent dielectric constant of single crystal $Ho_2Ti_2O_7$ measured in the presence of 0 T and 5 T magnetic field along (100) and (111) directions. (b) Magnitude of magnetocapacitance at 5 T along (100) direction (left axis) and square of magnetization (right axis) as a function of temperature. [93]

To uncover the physics of the multiferroic behavior of these geometrically frustrated ferromagnetic systems Lin et al. [88], performed temperature and magnetic field dependent pyroelectric study on polycrystal DTO. In temperature dependent dielectric permittivity they observed two dielectric relaxations at ~13 K and ~25 K, respectively showing the presence of two ferroelectric transitions in DTO. To confirm the ferroelectric transition they had performed temperature dependent pyroelectric measuremnts. Figure 1.28 shows the temperature dependent dielectric, pyroelectric current, and polarization of DTO. The

identical nature of electric polarization obtained from pyrocurrent measured at different warming rate suggests that the observed peak in pyroelectric measurement is associated with the electrical polarization.

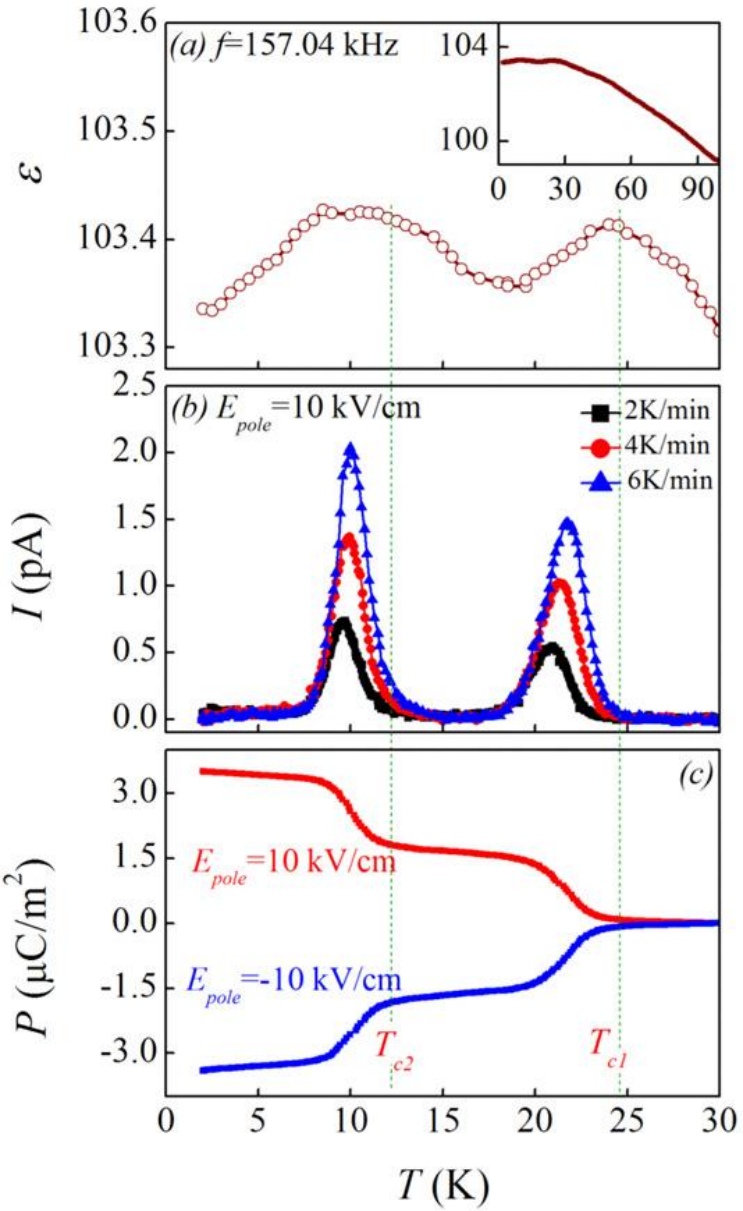

Figure 1.28: For $Dy_2Ti_2O_7$, (a) Temperature dependent dielectric constant (ε) measured at frequency 157 Hz. (b) Temperature dependent pyroelectric current under a series of warming rates. (c) Variation of electric polarization as a function of temperature after poling in positive and negative electric fields. [88]

To investigate the possible origin of both ferroelectric transition, they performed the temperature dependent pyroelectric current and polarization measurement at different magnetic field as shown in figure 1.29. It has been found that applied magnetic field affects only 13 K ferroelectric transition whereas 25 K ferroelectric transition remains unaffected. The so observed dependency of 13 K ferroelectric transition confirms that 13 K ferroelectric transition is associated with complex magnetism whereas 25 K ferroelectric transitions have structural origin.

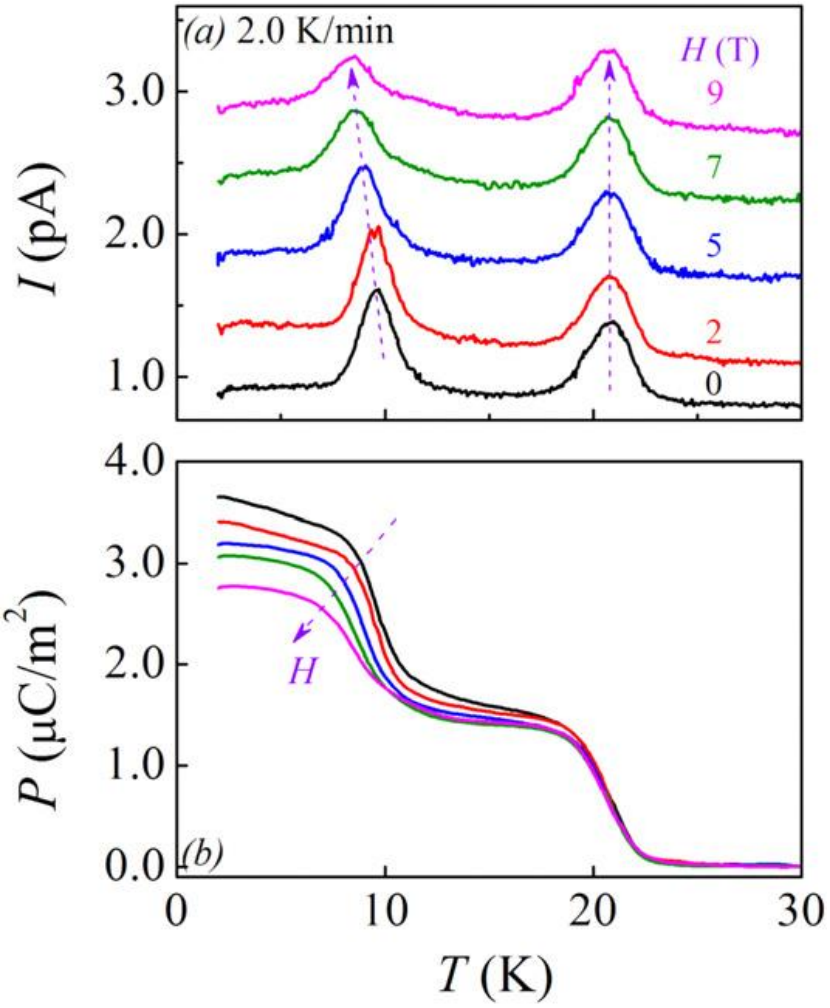

Figure 1.29: (a) pyroelectric current and (b) electric polarization at different magnetic field, as a function of temperature for $Dy_2Ti_2O_7$. [88]

Further, temperature dependent pyroelectric study performed on Dy site substituted Tb and Gd-doped DTO shows the suppression in both pyroelectric peaks suggesting the Dy-site related ferroelectric transition in these compounds. A similar finding was previously observed by Satio et al. [90], in low temperature magnetodielectric study performed on single crystal DTO. Figure 1.30 shows the variation in the magnetostriction as a function of magnetic field measured along (100) and (111) direction a different temperature. It has been noted that along (100) crystallographic direction measurement an increment in the magnetostriction has been observed with increasing magnetic field strength. Whereas, along (111) crystallographic direction measurement an anomaly at ~1 T has been observed which get shifted towards higher higher magnetic field on increasing temperature. From these observations Satio et al. concludes that observed magnetoelectric peak associated with the polarized 3in-1out spin structure.

These findings show that in HTO and DTO multiple ferroelectric transitions takes place in different temperature regime. Presence of ferroelectricity in these cubic compounds having space group $Fd\bar{3}m$, necessary implies symmetry lowering from cubic $Fd\bar{3}m$ down to a non-centrosymmetric space group (tetragonal, trigonal or lower), which must have a lattice effect such as-coupling of symmetry-breaking macroscopic strains or anomaly in anisotropic thermal parameters across the transitions, etc. In temperature dependent structural analysis there is no evidence of any structural transition is observed [87], [94]. A similar observation is reported by Saha et al. [95] and Mączka et al. [96], in their low temperature Raman study performed on HTO and DTO. In Raman study, no evidence of any structural transitions in HTO and DTO has been found. However, on decreasing temperature, mainly below 120 K, some anomalous softening in some of the phonon modes are observed in both compounds.

Their analysis concludes that these softening is associated with the structural distortion in the oxygen positions.

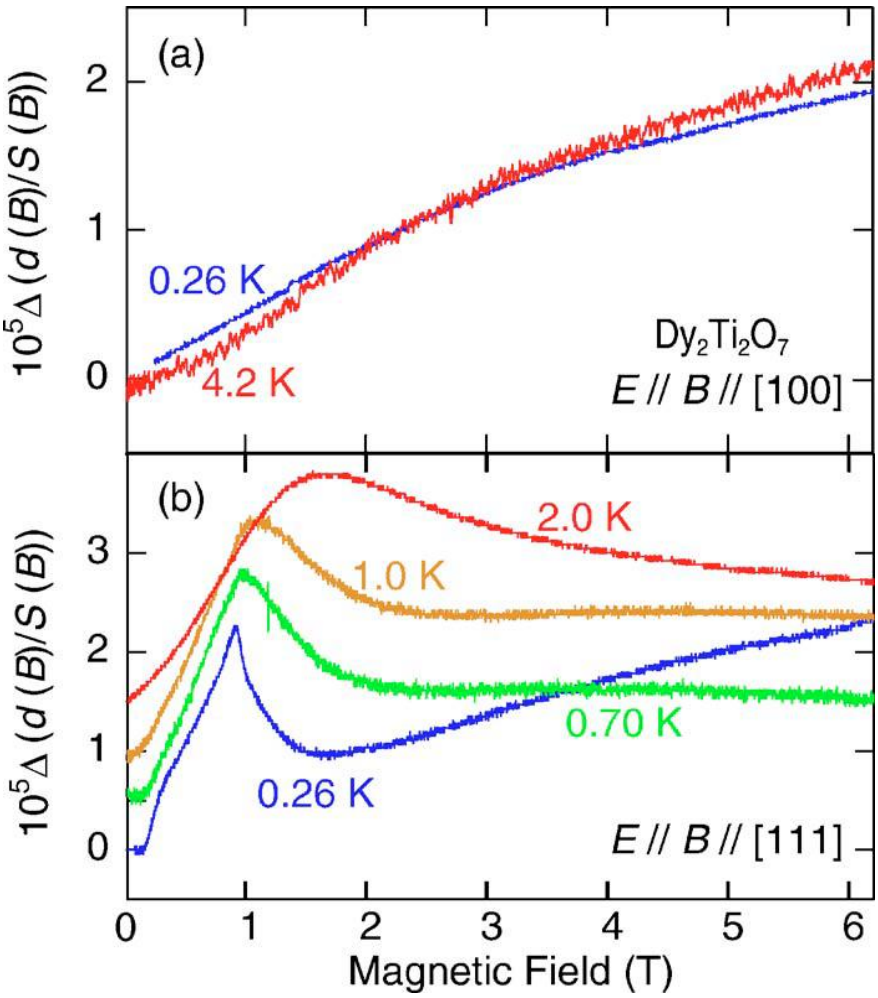

Figure 1.30: Magnetostriction in $Dy_2Ti_2O_7$ along (a) (100) and (b) (111) crystallographic direction. d(B) and S(B) representing the thickness and area of the sample in the presence of magnetic field (B). [90]

Furthermore, symmetry analysis of cubic $Fd\bar{3}m$ space group is suggesting the incompatibility of structural order parameters with gyrotropic order which belongs to the A_{1u} irreducible representation of the O_h point group [97]. This means that in these cubic compounds

emergence of ferroelectricity can have only an electronic origin instead of structural origin. However, the factors responsible for the emergence of multiple ferroelectric transitions and its associated nature are still unknown and a matter of investigation.

1.8 Objectives of the thesis

On the basis of these observations, the objective of the present Ph.D. thesis is

- Study of nature and origin of ferroelectric transitions in $Ho_2Ti_2O_7$ and $Dy_2Ti_2O_7$.
- Investigation of parameters affecting the spin dynamics in these frustrated compounds.
- Study the nature of fluctuation (quantum/classical), driving the spin dynamics at low temperature and effect of magnetic perturbations in $Ho_2Ti_2O_7$ and $Dy_2Ti_2O_7$.
- Study the quantum correlation and its associated scrambled quantum information in quantum critical region in $Ho_2Ti_2O_7$ and $Dy_2Ti_2O_7$.